

**OPEN ACCESS**

## Review—Lab-in-a-Mouth and Advanced Point-of-Care Sensing Systems: Detecting Bioinformation from the Oral Cavity and Saliva

To cite this article: Chochanon Moonla *et al* 2022 *ECS Sens. Plus* 1 021603

View the [article online](#) for updates and enhancements.



# Review—Lab-in-a-Mouth and Advanced Point-of-Care Sensing Systems: Detecting Bioinformation from the Oral Cavity and Saliva

Chochanon Moonla,<sup>1,\*,\*</sup> Don Hui Lee,<sup>3,4,=</sup> Dinesh Rokaya,<sup>5</sup> Natcha Rasitanon,<sup>1,2</sup>  
Goma Kathayat,<sup>6</sup> Won-Yong Lee,<sup>3</sup> Jayoung Kim,<sup>4,z</sup> and Itthipon Jeerapan<sup>1,2,\*,z</sup>

<sup>1</sup>Center of Excellence for Trace Analysis and Biosensor, Prince of Songkla University, Hat Yai, Songkhla 90110, Thailand

<sup>2</sup>Division of Physical Science and Center of Excellence for Innovation in Chemistry, Faculty of Science, Prince of Songkla University, Hat Yai, Songkhla 90110, Thailand

<sup>3</sup>Department of Chemistry, Yonsei University, Seoul 03722, Republic of Korea

<sup>4</sup>Department of Medical Engineering, College of Medicine, Yonsei University, Seoul 03722, Republic of Korea

<sup>5</sup>Department of Clinical Dentistry, Walailak University International College of Dentistry, Walailak University, Bangkok 10400, Thailand

<sup>6</sup>Department of Biochemistry, Manipal College of Medical Sciences and Teaching Hospital, Pokhara, Nepal

*Cavitas* sensors and point-of-need sensors capable of providing physical and biochemical information from the oral cavity and saliva have attracted great attention because they offer remarkable advantages for noninvasive sensing systems. Herein, we introduce the basic anatomy and physiology of important body cavities to understand their characteristics as it is a pivotal foundation for the successful development of in-mouth devices. Next, the advanced development in lab-in-a-mouth sensors and point-of-need sensors for analyzing saliva are explained. In addition, we discuss the integrations of artificial intelligence and electronic technologies in smart sensing networks for healthcare systems. This review ends with a discussion of the challenges, future research trends, and opportunities in relevant disciplines. Mouthguard-based sensors and conventional salivary sensing devices will continue to be significant for the progress in the next-generation sensing technologies and smart healthcare systems.

© 2022 The Author(s). Published on behalf of The Electrochemical Society by IOP Publishing Limited. This is an open access article distributed under the terms of the Creative Commons Attribution 4.0 License (CC BY, <http://creativecommons.org/licenses/by/4.0/>), which permits unrestricted reuse of the work in any medium, provided the original work is properly cited. [DOI: 10.1149/2754-2726/ac7533]



Manuscript submitted May 18, 2022; revised manuscript received May 30, 2022. Published June 27, 2022.

## Introduction and a Brief History of Lab-in-a-Mouth and Advanced Point-of-Care Sensing Systems for Examining the Oral Cavity and Saliva

Human saliva is an oral fluid that is transparent, multi-constituent, and mildly acidic (pH 6.0–7.0). Saliva is produced by several salivary glands, including the submandibular, parotid, and sublingual glands, and contains secretions from other small glands under the oral mucosa and periodontal tissues.<sup>1</sup> Oral fluid makes food swallowing, oral digestion, tissue lubrication, tooth care, and antiviral and antibacterial defense easier.<sup>2</sup> Saliva is a complex combination of 99.5% water and 0.5% electrolyte, metabolites, mucus, peptides, enzymes, glycoprotein, and antibacterial compounds (such as immunoglobulin A and lysozyme).<sup>3</sup> Saliva can be used as a diagnostic tool for mimicking both oral and systemic health issues, as well as for recognizing gastroesophageal reflux disease occurrences, thanks to advances in bioinformatics, proteomics, and genomes.<sup>4,5</sup> Advantageously, saliva sampling avoids the risks of infection that might occur with blood testing and is a cost-effective technique to screen large populations. Furthermore, saliva has a strong association with blood levels of several indicators due to the direct penetration of elements from blood to saliva via transcellular or paracellular pathways.<sup>6</sup> As a result, oral fluid is a viable alternative to intrusive blood analysis, and the medium may be used to monitor health and disease.<sup>7</sup> Many biomarkers generated by activated inflammatory cells, such as tumor necrosis factors, interleukins, and chemokines, are found in the oral cavity and might be used to diagnose, prevent, and treat chronic illnesses.<sup>8,9</sup> Furthermore, the mouth cavity contains many antioxidants, which operate as a protective barrier against oxidative stress induced by inflammation and bacteria. These biomarkers also reflect human

health, ranging from oral disorders (e.g., periodontitis oral cancer) to systemic diseases (e.g., diabetes and rheumatoid arthritis).<sup>10–12</sup>

The oral cavity could be a promising body part for getting a variety of health information from gum, teeth, and saliva. The first oral status monitoring device on a partial denture was conducted by Graf in the 1960s to monitor pH and fluoride ion levels.<sup>13,14</sup> However, when the sensor operates in the oral cavity, there is no consideration to confirm if there is any adverse effect on the body, and there was a risk that the internal solution of the device may leak out. Biosensors using wearable platforms, including wearing oral cavity, have further developed rapidly since 2010. Figure 1 depicts a brief history of biosensing technology before today's wearable biosensors including some PoC devices.<sup>13–34</sup> These achievements opened the way for current wearable biosensors for noninvasive biomonitoring applications as a replacement for blood monitoring biomedical equipment in a variety of healthcare applications. In 2012, Mannoor et al. printed graphene on water-soluble silk and then transferred it onto bovine tooth enamel to develop an intraoral wearable bacterial detection device that functioned for wireless monitoring by using its resonant circuit-based nature.<sup>16</sup> They demonstrated conformability by transferring the bacterium sensor to a tooth in vitro, which might cause the graphene sensor's impedance to alter. Since then, significant efforts have been made on developing oral wearable biosensors which can monitor the health status of the wearer in saliva, mainly those targeting metabolites. In addition to these oral wearable devices, diverse types of lateral flow, and paper-based strips,<sup>15</sup> based sensors were developed in a colorimetric or electrochemical disposable form based on saliva's usefulness for health monitoring. In the 2010s, these PoC devices were mainly developed to be connected to smartphones to read measurement signals, allowing them to be measured directly with smartphones owned by users without the need for professional equipment. Users can obtain quantitative information if the user reads electrical signals with the smartphone or if the user reads out optically using their smartphone's camera. Lateral flow, especially in the case of a colorimetric device, has the advantage of obtaining qualitative

\*Equal Contribution.

\*Electrochemical Society Member.

<sup>z</sup>E-mail: [jayoungkim@yonsei.ac.kr](mailto:jayoungkim@yonsei.ac.kr); [itthipon.j@psu.ac.th](mailto:itthipon.j@psu.ac.th)

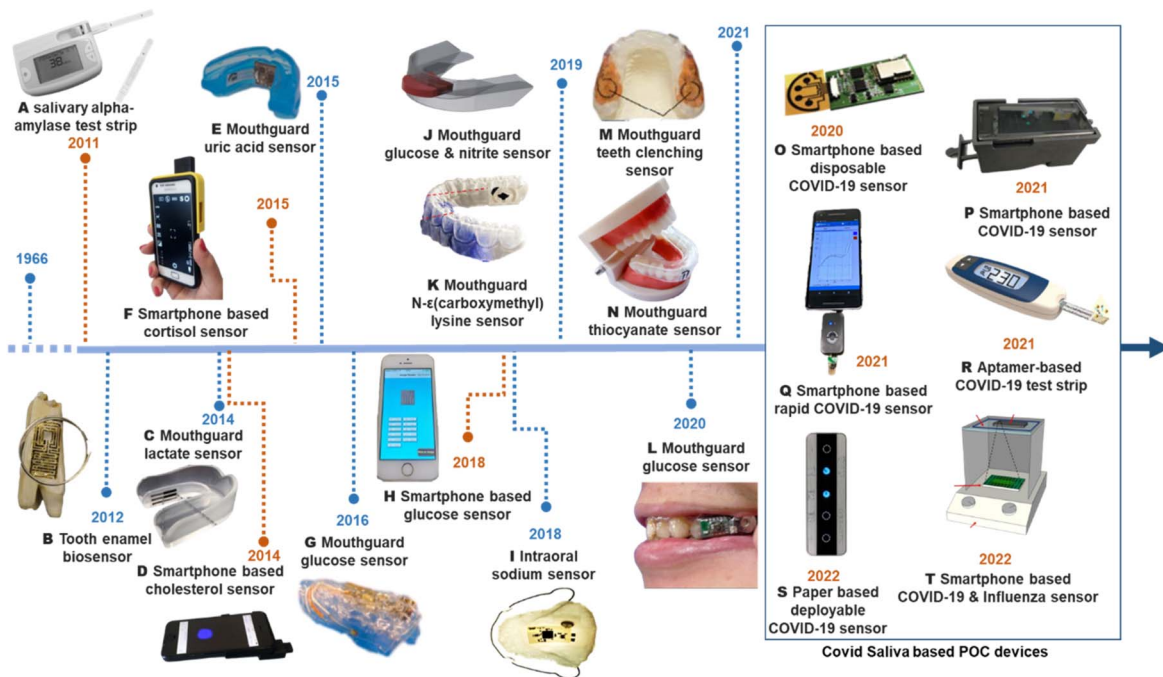


**Figure 1.** The representative timeline of key advances in PoC sensors for saliva analysis and *cavitas-oris* sensors. (A) salivary  $\alpha$ -amylase test strip. Adapted with permission,<sup>15</sup> Copyright 2011, Elsevier. (B) Tooth enamel biosensor. Adapted under the terms and conditions of the CC-BY 4.0,<sup>16</sup> Copyright 2012, Mannoor, Manu S., et al., published by *Nature Communications*. (C) Mouthguard lactate sensor. Adapted with permission,<sup>17</sup> Copyright 2014, the Royal Society of Chemistry. (D) Smartphone-based cholesterol sensor. Adapted with permission,<sup>18</sup> Copyright 2014 American Chemical Society. (E) Mouthguard uric acid sensor. Adapted with permission,<sup>19</sup> Copyright 2015, Elsevier. (F) Smartphone-based cortisol sensor. Adapted with permission,<sup>20</sup> Copyright 2015, Elsevier. (G) Mouthguard glucose sensor. Adapted with permission,<sup>21</sup> Copyright 2016, Elsevier. (H) Smartphone-based glucose sensor. Adapted with permission,<sup>22</sup> Copyright 2018, Springer Nature. (I) Intraoral sodium sensor. Adapted under the terms and conditions of the CC-BY 4.0,<sup>23</sup> Copyright 2018, Lee, Yongkuk, et al., published by *Proceedings of the National Academy of Sciences*. (J) Mouthguard glucose and nitrite sensor. Adapted with permission,<sup>24</sup> Copyright 2019, Springer Nature. (K) Mouthguard N- $\epsilon$ (Carboxymethyl)lysine sensor. Adapted with permission,<sup>25</sup> Copyright 2019, Elsevier. (L) Mouthguard glucose sensor. Adapted with permission,<sup>26</sup> Copyright 2020 American Chemical Society. (M) Mouthguard teeth clenching sensor adapted under the terms and conditions of the CC-BY 4.0,<sup>27</sup> Copyright 2021, Kinjo et al., published by *Sensors*. (N) Mouthguard thiocyanate sensor. Adapted with permission,<sup>28</sup> Copyright 2021, Springer Nature. (O) Smartphone-based disposable COVID-19 sensor. Adapted with permission,<sup>29</sup> Copyright 2020, Elsevier. (P) Smartphone-based COVID-19 sensor. Adapted under the terms and conditions of the CC-BY 4.0,<sup>30</sup> Copyright 2021, Ning, Bo, et al., published by *Science Advances*. (Q) Smartphone-based rapid COVID-19 sensor. Adapted with permission,<sup>31</sup> Copyright 2021, Elsevier. (R) Aptamer-based COVID-19 test strip. Adapted with permission,<sup>32</sup> Copyright 2021, Elsevier. (S) Paper-based deployable COVID-19 sensor. Adapted with permission,<sup>33</sup> Copyright 2022, Elsevier. (T) Smartphone-based COVID-19 and Influenza sensor. Adapted under the terms and conditions of the CC-BY 4.0,<sup>34</sup> Copyright 2022, Heithoff, Douglas M., et al., published by *JAMA network open*.

information, but there is a limitation in accuracy in determining the degree of color change and using it for quantitative use. On the other hand, the PoC device is still limited to single-use, and continuous monitoring in daily life. With the development of wearable technology, it is possible to introduce miniaturization, flexibility, and wireless communication modules; saliva PoC will also be translated into wearables.

In 2014, the first mouthguard biosensor was reported to analyze salivary lactate, a type of biomarker associated with physical stress and performance.<sup>17</sup> In 2015, the same group developed the next generation of mouthguard biosensor integrated wireless equipment that can measure salivary uric acid, a biomarker related to hyperuricemia.<sup>19</sup> In 2016, a denture-shaped, salivary glucose biosensor was developed that was worn on the back tooth, smaller than the mouthguard form factor, and tested in a phantom-jaw system mimicking an oral environment.<sup>21</sup> In 2020, the same group further developed a salivary glucose biosensor on a mouthguard employing the cellulose acetate membrane to filter out unnecessary obstructive substances from saliva and demonstrated the application in vivo with human subjects.<sup>26</sup> Additionally, a mouthguard sensor that can measure two biomarkers, including glucose and nitrite, at the same time was developed. Although it has the advantage of being able to measure two biomarkers at the same time, this sensor is a colorimetric sensor and has a disadvantage in that the colorimetric response can be checked while the sensor is detached from the mouth, since it does not have wireless readout electronics, but it requires naked-eye detection.<sup>24</sup> In addition to oral wearable devices for metabolites, various devices for other chemical compounds such as electrolytes have

also been developed.<sup>35</sup> In 2017, wearable salivary sensors were expanded to measure pH change in the oral cavity, a biomarker associated with periodontal disease and such as enamel decalcification.<sup>36</sup> In 2018, a *cavitas* sensor that measured salivary sodium, a type of electrolyte while consuming food in vivo, was developed.<sup>23</sup> In 2019, the target biomarkers were further expanded to N-carboxymethyl-lysine and 3-Nitro-L-tyrosine which associated with diabetes and atherosclerotic, long-term damage to proteins in aging, and oxidative stress.<sup>25,37</sup> In 2021, the salivary thiocyanate sensor was integrated with a mouthguard.<sup>28</sup> Thiocyanate in the saliva is very much related to smoking, and by monitoring it, smokers and nonsmokers can be distinguished. The mouthguard wearable platform was utilized not only for salivary biosensors, but also for physical sensors, which is capable of monitoring physical teeth clenching.<sup>27</sup> From the 2010s to recent years, wearable devices have been significantly developed to monitor healthcare-related various parameters in the oral cavity.

In the 2010s, salivary PoC devices also made many advances like intraoral wearable biosensors. Many examples of integrating the signal reader with sensors (such as the  $\alpha$ -amylase test-strip sensor) were reported in 2011. These examples could read the signals using smartphones.<sup>18,20,22</sup> As the coronavirus disease 2019 (COVID-19) started to spread worldwide in late 2019, salivary PoC devices began to develop faster.<sup>38</sup> Faced with the challenges of rising hospital visits, clinic/laboratory testing, and complying with the social distancing recommendation to reduce the risk of disease spread, these facts demonstrated the emerging need for mobile sensing and biosensing technologies in future sustainable healthcare systems.

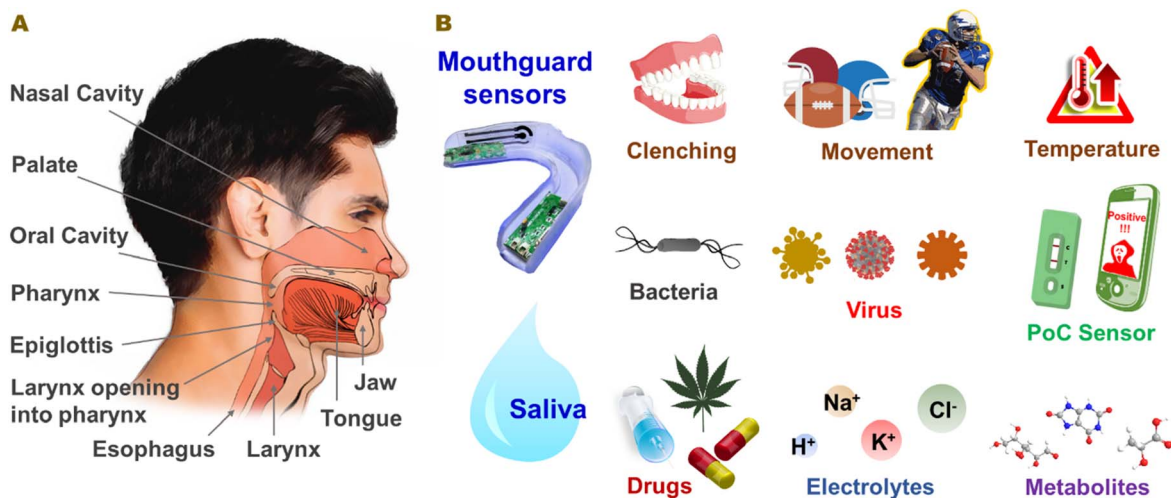


**Figure 2.** (A) Anatomy of important cavities and (B) the concept of lab-in-a-mouth and point-of-need sensors.

Therefore, many studies have been focused on the COVID-19 diagnosis method using noninvasive saliva that can be used instead of the examination method utilizing invasive blood collection, which requires medical personnel. As a part of the development of these diagnostic methods, point-of-care (PoC) has been developed to immediately monitor the presence of COVID-19 infection through biomarkers in saliva. In 2020, PoC devices capable of rapid and low-cost COVID-19 diagnosis were reported by measuring viral antigen nucleocapsid protein, immunoglobulin M (IgM), and immunoglobulin G (IgG) antibody, as well as inflammatory biomarker C-reactive protein.<sup>29</sup> This multiplexed immunosensor device might enable COVID-19 telemedicine diagnosis and monitoring with high-frequency at-home testing. In 2021, there were PoC sensors based on smartphones, which read the fluorescence generated by loading and reacting saliva lysate into the recombinase polymerase amplification (RPA)-CRISPR solution preloaded chip with a smartphone.<sup>30</sup> It has also been reported that a biosensor modified with human receptor angiotensin-converting enzyme-2 (ACE2) can detect SARS-CoV-2 with 10 l of a sample in 4 min using electrochemical impedance spectroscopy.<sup>31</sup> In the same year, SARS-CoV-2 salivary antigen assay, which also being read with an aptamer-based glucose meter, was reported.<sup>32</sup> In 2022, a loop-mediated isothermal amplification assay method capable of detecting SARS-CoV-2 and influenza viruses based on smartphones was developed;<sup>34</sup> moreover, another paper-based biosensor could detect SARS-CoV-2 RNA in human saliva, representing another example of a visual bioluminescent biosensor.<sup>33</sup> For the diagnosis of COVID-19, disposable salivary PoC devices have already offered benefits by taking advantage of easy saliva sampling. Although such PoC devices require an additional saliva sampling process, COVID-19 diagnostics do not require very frequent (e.g., hourly) or continuous assessment. Thus, a disposable PoC device type can be enough for virus detection. But later, for various health indicators, including COVID-19, a multimodal sensing system as a wearable device could be exploited for daily life monitoring.

In this article, we critically review recent progress in the development of intraoral wearable sensors and the potential usefulness of saliva and oral cavity for healthcare applications (Fig. 2), along with addressing future challenges to overcome.

### Introduction to Anatomy of Oral Cavities and Functions of Saliva

Oral and nasal cavities act as channel exterior environments of human systems (Fig. 2A).<sup>39</sup> These nasal and oral cavities are the entry points of the respiratory system and digestive system, respectively.<sup>40</sup> The structures and functions of the oral cavity work

in an analogous way to a machine that follows the laws of both physics and chemistry for its function. The facial bones form the backbone of the oral cavity and its associated structures. The maxilla forms the middle-third of the face and is joined together in the midline forming the intermaxillary suture.<sup>41</sup> Mandible forms the lower third of the face. The alveolar process of the maxilla and mandible forms sockets where the teeth are embedded with the help of periodontal ligaments. The temporomandibular joints (TMJ) are the two hinge joints that connect the mandible to the skull through the temporal bone. The disc and both bony areas of the joint are intricately held together by the muscles of mastication, and their associated tendons and ligaments. There are joints that slide and rotate and help to move the lower jaw (mandible) up and down and side to side and help in various functions such as chewing, swallowing, and speaking. The groups of muscles that help in the mastication, speech, and swallowing are muscles of mastication (masseter, temporalis, medial pterygoid, and lateral pterygoid), suprahyoid muscles, muscles of facial expression, and tongue.<sup>41</sup>

**Oral cavity.**—The oral cavity (mouth) includes the lips, inside lining of the cheeks and lips, palate, upper and lower gums, anterior 2/3 of the tongue, the floor of the mouth, and retromolar (area behind the last molars).<sup>42</sup> The oral mucosa covers the oral cavity apart from the teeth and it consists of two layers: epithelium (surface layer) and lamina propria (corium, deeper layer). The oral mucosa helps in the protection of the inner tissues such as muscle, blood vessels, and nerves. It also provides mechanical protection against trauma during chewing, and protects against bacteria and toxic substances. The oral mucosa has taste buds for taste recognition. Epithelial cells have a high turnover rate and they can renew themselves after cells die.<sup>43</sup> The mature cells can transform into keratinized and nonkeratinized cells. The mucosa of the hard palate, gingiva, and bottom (dorsum) of the tongue is tough and resistant to abrasion, and tightly bound to underlying tissue.<sup>44</sup> Similarly, other cells found in oral mucosa include melanocytes, Langerhans cells, lymphocytes, and Merkel cells.

**Mastication.**—Mastication (chewing) is a functional activity that uses muscles, teeth, periodontal structures, lips, cheeks, palate, tongue, and salivary glands. It is automatic and involuntary which is made up of rhythmic actions. The central pattern generator, a pool of neurons, controls the mastication. A chewing stroke is divided into an opening phase and a closing phase.<sup>45</sup> During the opening and closing phases, there may be some lateral deviation toward the working side. The closing phase or movement is further subdivided into the crushing and grinding phase as shown in Fig. 3A.<sup>46</sup>



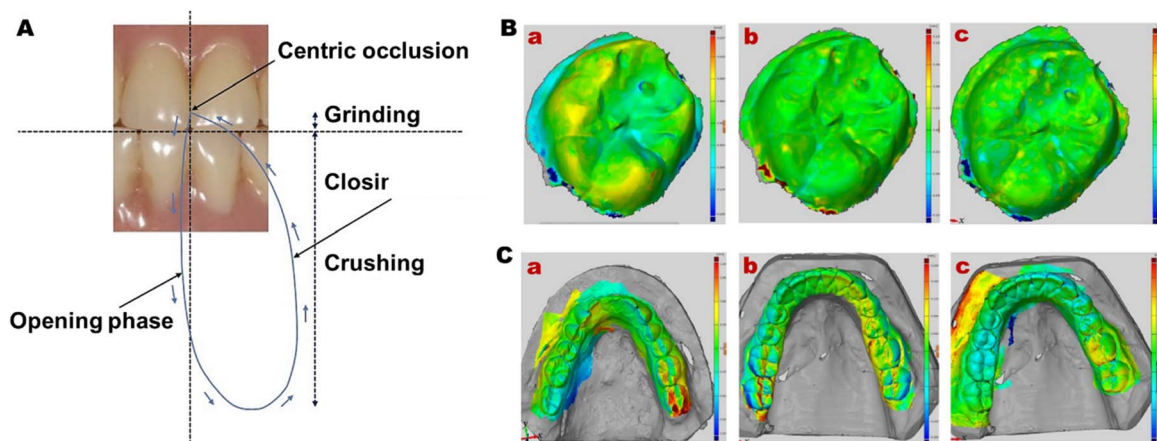


**Figure 3.** (A) Mastication and its cycle. Digital occlusal analysis of (B) deviation on a single unit and (C) deviation on the mandibular arch; (a) Zfx Intrascan, (b) Lava Cos, and (c) Trios 3-Shape. Adapted under the terms and conditions of the CC-BY 4.0,<sup>45</sup> Copyright 2016, Eneko Solaberrieta et al., published by *BioMed Research International*.

Swallowing is a sequence of organized muscular contractions which move the food bolus from the mouth to the stomach through the esophagus. Following the mastication, swallowing occurs. Swallowing is comprised of voluntary activity, involuntary activity, and reflex muscular activity. During swallowing the lips come in contact sealing the oral cavity, and teeth are in maximum contact (intercusation).

**Dental occlusion.**—Occlusion is the static (when the mandible is not moving) relationship between the maxillary or mandibular teeth. Alternatively, the dynamic relationship of the mandible to the maxilla occurs when the contact relationship between the teeth during function and mandibular movements.<sup>47,48</sup>

In the last decades, we observe a massive improvement in digital technology. The virtual environment has improved the diagnosis, treatment planning, and treatment of clinical cases. There are two methods for the analysis of occlusion in clinical settings: nondigital and digital (computerized).<sup>45</sup> Nondigital occlusal analysis consists of instruments such as articulating paper, wax, etc., whereas digital occlusal analysis consists of various digital instruments such as T Scan II Occlusal Analysis System, Biopak Electromyography Recording System,<sup>47</sup> and intraoral scanner.<sup>48</sup> The computerized occlusal analysis system shows the ability to provide measurable force and time variance in a real-time mode from the initial tooth contact into maximum intercusation.<sup>48</sup> In addition, the advantage of the computerized system is an improved occlusal indicator than the nondigital (convention) system as the computerized system accurately shows the occlusal contacts.

Through the computerized system, the occlusal condition of a dental prosthesis or natural teeth can be easily evaluated and quantified, and the quality of occlusal parameters and muscle activity can be also evaluated.<sup>49</sup> In addition, the system can be used to perform precise occlusal adjustment procedures in extensive restorative work with occlusal discomfort post-operatively and chronic myofascial pain dysfunction syndrome.<sup>45</sup>

The limitation of a digital occlusal record is the costs and deviation of the digital or virtual occlusal record (Figs. 3B–3C). Deviation in recording the digital occlusal depends on various factors, such as accuracy of the machine or scanner, alignment, and size of the record.<sup>41,42</sup>

**Saliva.**—Saliva is a unique biological fluid and has a vital role in the human body. Salivary glands produce saliva. Major salivary glands include parotid, submandibular, and sublingual glands which are paired.<sup>50</sup> In addition, most oral mucosal surfaces have minor mucus-secreting salivary glands. The openings of the Wharton ducts, which drain the ipsilateral submandibular and sublingual glands lie

near the midline on each side of the floor of the mouth, whereas the parotid glands via the Stensen’s ducts drain into the cheeks.<sup>50</sup>

The composition of saliva includes water, proteins, mucus, mineral salts, and amylases.<sup>51</sup> Various proteins present in saliva have an important physiological role in the human body as shown in Table I.<sup>50–52</sup>

The composition of saliva and saliva flow rate responds to the parasympathetic or sympathetic innervations. Low salivary flow with high protein is produced under the influence of sympathetic impulses while high salivary flow with low protein is produced under influence of parasympathetic impulses.<sup>54</sup> Salivary amylases indicate sympathetic nervous system activity. In addition, various PoC devices are designed to detect the status of saliva and they can be employed for self-reported psychological states.<sup>55</sup>

In recent years, we notice a surge of interest in saliva as a diagnostic fluid.<sup>54</sup> Many indicators in saliva are immediately transferred from the blood through transcellular or paracellular pathways, making saliva a “mirror of the human body” that reflects the physiological status of the body and provides a noninvasive alternative to blood examination. Saliva is a complex oral fluid made up of various ingredients such as metabolites, ions, proteins, and hormones that are produced mostly by the salivary gland.<sup>55–61</sup> Several biomarkers (e.g., drugs, hormones, metabolites, and proteins) have been employed in clinical situations because they provide useful diagnostic information.<sup>57,62–65</sup> Salivary chemicals comprise a diverse range of biological agents, including salivary gland-produced substances, exogenous substances, bacteria, and blood-permeating substances. Saliva testing, on the other hand, has drawbacks when compared to blood analysis. The quantities of biomarkers in saliva are frequently many orders of magnitude lower than in blood. Next, there are unknown areas regarding the correlation between biomarker levels in saliva and serum. We should consider background noise, interferences, matrix effects, viscosity, salivary flow rate, and food consumption for establishing accurate and stable saliva testing.

Metabolites, electrolytes, proteins, and hormones are significant examples of biomarkers found in saliva. First, Shibasaki et al.<sup>66</sup> and Soukup et al.<sup>67</sup> stated that the metabolites include uric acid, lactate, glucose, bilirubin, cholesterol, and creatinine; the report shows that in the case of uric acid, the relationship between blood uric acid level and salivary uric acid level shows a strong association. Uric acid levels that are abnormal are biomarkers for a variety of disorders, including hyperuricemia, gout, renal syndrome, and Lesch-Nyhan syndrome.<sup>68–72</sup> Kim et al.<sup>19</sup> reported a wearable salivary uric acid mouthguard biosensor with integrated wireless electronics that uses the features of salivary uric acid concentration. By monitoring the salivary uric acid level of healthy people and those with

**Table I. Various salivary protein constituents and their role in the human body.**<sup>50,52,53</sup>

Salivary proteins	Functions
Histatins	These polypeptides are present only in saliva which have anti-bacterial and anti-fungal activities.
Proline-rich proteins (PRPs)	Acidic PRPs are found only in saliva whereas the basic PRPs are also found in other secretions.
Mucins	These are glycoproteins and have specific tissue distributions and amino acid sequences. They provide the viscoelastic character of the mucosal secretions.
Lysozyme	They have a role in the ancient self-defense system.
Immunoglobulin A (IgA)	They have a role in the sophisticated adaptive immune system.
Cystatin	They belong to a multigene family.
$\alpha$ -Amylase	They play a specific role in digestion but are also present in several body fluids.
Albumin and kallikrein	They are components of blood plasma. Albumin circulates into the different mucosal secretions and kallikrein is secreted exclusively by the mucosal glands.

hyperuricemia in real-time, researchers discovered that the level of salivary uric acid reduces during hyperuricemia patients' therapeutic treatment. Additionally, the same group measured salivary lactate level, which has a good correlation with blood lactate and hence can indicate a person's physical stress.<sup>17,73,74</sup> Salivary glucose was utilized for noninvasive monitoring of diabetes based on the correlation with blood level. According to Soni et al.,<sup>75</sup> the correlation between saliva and blood in diabetes patients is about  $R = 0.95$ . As a result, in diabetes patients, measuring salivary glucose instead of blood glucose may be useful for diabetes patients. The salivary glucose concentration could be detected (instead of the blood glucose concentration) and utilized as a biomarker for diabetes patients. Therefore, wearable sensors to assess the salivary glucose level have been created.<sup>26,76,77</sup> Bilirubin is another biomarker found in human saliva, and low bilirubin levels are linked to coronary artery infections and anemia. In extreme cases, excessive bilirubin concentrations can cause biliary duct or hepatic malfunction, as well as brain damage and death.<sup>78–80</sup> As a result, the bilirubin level can be utilized as a useful guideline for detecting a variety of liver illnesses. Hyperbilirubinemia is defined as high bilirubin levels in the blood (more than  $2.5 \text{ mg dl}^{-1}$ ) in the presence of jaundice. There is a correlation between salivary and serum bilirubin levels in identifying newborn jaundice, according to one study.<sup>81</sup> A recognition sensor based on molecularly imprinted polymer (MIP) that monitors bilirubin in saliva has been published.<sup>82</sup> Although most salivary lipids are glandular in origin, some may have disseminated directly from serum. Karjalainen et al. studied the quantity of cholesterol in healthy people's saliva and found that the concentration of cholesterol in saliva resembles the serum cholesterol level to some extent.<sup>83</sup> In the serum and saliva of 100 healthy volunteers, Singh et al. found a moderate association between high-density lipoprotein (HDL) cholesterol, triglycerides (TC), and very-low-density lipoprotein (VLDL) cholesterol.<sup>84</sup> Low cholesterol amounts in saliva can be measured using an enzymatic sensor.<sup>85</sup> Creatinine levels can be raised by infections and malignant disorders like cancer.<sup>86</sup> Untreated symptoms can lead to progressive engorgement of nephrons, resulting in final-stage chronic kidney disease (CKD).<sup>87</sup> The pathogenic mechanism of advanced kidneys includes cellular destruction, podocyte damage, inflammation, and glomerulus hypertrophy. The salivary and serum creatinine levels had a substantial positive connection ( $R = 0.82$ ).<sup>88</sup> For PoC detection of advanced renal illnesses, a stress-free electrochemical-based sensor with an Internet of Things (IoT) device for salivary creatinine assessment was developed. Noninvasive monitoring of creatinine levels in saliva might provide useful and real-time data for preventive diagnosis and therapeutic evaluation of CKD at various stages and renal dysfunction.<sup>89</sup>

Sodium, potassium, calcium, chlorine, fluoride, ammonia, and other electrolytes fall into the second category. There were no significant relationships between saliva and plasma levels of sodium, potassium, or calcium.<sup>90</sup> Although sodium in the saliva is not a biomarker for a specific disease, high salt intake is linked to an increased risk of fatal or otherwise severe cardiovascular illness, given the well-known link between the risk of cardiovascular disease and high blood pressure. All adults, including the elderly, should take fewer than 2000 mg of sodium or 5 grams of salt per day, according to the World Health Organization (WHO). Long-range wireless telemetry has also been used to construct an oral monitoring device for sodium consumption.<sup>23</sup> Graf introduced the first salivary pH<sup>13</sup> and ion<sup>14</sup> detection device in a wearable platform on a partial denture to monitor fluoride ion levels in the 1960s. Fluoride is a biologically important anion that plays a vital function in oral health and osteoporosis.<sup>91</sup> Oliveby A et al.<sup>92</sup> discovered that the fluoride content in entire saliva was similar to that in plasma, although at a lower level. The salivary fluoride level was unaffected by changes in salivary flow rate. As a result, the original fluoride level might be employed as a fluorosis biomarker. Salivary pH is a key determinant in dental illnesses such as enamel decalcification, according to a few studies,<sup>93,94</sup> and it is easy to measure for quick clinical evaluations.

Proteins, such as  $\alpha$ -amylase, albumin, secretory-immunoglobulin A (IgA), and Lysozyme, fall into the third category. Salivary  $\alpha$ -amylase has also emerged as a novel biomarker of the sympathetic nervous system's reactivity to psychosocial stress,<sup>95</sup> which is secreted by the salivary gland in response to adrenal activity and suppressed by  $\beta$ -blockade.<sup>96</sup> An  $\alpha$ -amylase secretion is induced by acute experimental stressors,<sup>97–99</sup> whereas chronic stress may be linked to lower  $\alpha$ -amylase output.<sup>100</sup> An  $\alpha$ -amylase has an endogenous diurnal cycle and is independent of the salivary flow rate.<sup>101</sup> Although the physiological importance of salivary  $\alpha$ -amylase release in response to stress is unknown, it could be a valuable indicator of stress-related autonomic activity.<sup>102</sup> Hsiao, Hsien-Yi, et al.<sup>103</sup> reported a hand-held colorimetric sensor platform for measuring salivary  $\alpha$ -amylase activity. Salivary albumin levels are higher in hemodialysis patients, and changes in hemodialysis patients' health, such as hyperparathyroidism, appear to have an impact on salivary composition.<sup>104</sup> Hemodialysis patients had higher salivary albumin concentrations ( $0.10 \pm 0.06 \text{ g dl}^{-1}$ ) than healthy people ( $0.05 \pm 0.03 \text{ g dl}^{-1}$ ). Salivary albumin levels could be employed as a biomarker in cases of oral squamous cell carcinoma; however, they may not be effective as a biomarker for early diagnosis of chronic generalized periodontitis, according to Koduru, Mallikarjuna Rao, et al.<sup>105</sup> Furthermore, salivary albumin is an important component in the diagnosis and prognosis of type 2 diabetes and oral cancer.<sup>106–108</sup> Concentrations of Salivary secretory immunoglobulin A may represent the health of the body, including the presence of malignancies, as a stress sign, and as indicators of general body condition.<sup>109</sup> The example highlights the need of keeping track of salivary secretory immunoglobulin A levels in the body. The sensitive salivary immunoglobulin biosensor was developed using nanomaterials. Rizwan, Mohammad, and colleagues<sup>110</sup> described an immunosensor that can detect secretory immunoglobulin A in saliva samples. Lysozyme is a key innate immune defense molecule and one of the primary proteins in saliva, with levels ranging from 1.4 to  $28 \mu\text{M}$ .<sup>111,112</sup> Lysozyme is a clinically relevant protein because its levels rise in monocytic and monomyelocytic leukemia, tuberculosis, rapid bacterial infections, and monocytosis associated with inflammatory bowel disease.<sup>112</sup> Di Giulio, Tiziano, and colleagues<sup>113</sup> developed electrochemical salivary lysozyme biosensors using molecularly imprinted polymer for chronic illness monitoring.

Salivary hormones, the fourth classification, cortisol can be a representative biomarker.<sup>114</sup> Salivary cortisol measurement is physiologically important because it closely mirrors unbound cortisol levels in the blood. Cortisol rises in response to stress, making it a stress biomarker.<sup>58,115</sup> Salivary cortisol has a strong correlation with free blood cortisol because it is unaffected by transport methods or the type, quantity, or quality of saliva.<sup>58,115</sup> In a healthy person, salivary cortisol levels should be between 1 and  $10 \text{ ng ml}^{-1}$ .<sup>116</sup> Shima Dalirirad et al.<sup>116</sup> created a disposable biosensor to detect salivary cortisol by using aptamer as a recognition element of the sensor at the PoC. This easy and quick approach detects cortisol levels in the  $0.5\text{--}15 \text{ ng ml}^{-1}$  range. Testosterone is a unique steroid hormone that serves as the principal androgen. This hormone is mostly secreted by the reproductive organs and has an important function in human health. Testosterone levels vary with age, with an average value of  $2.01\text{--}7.5 \text{ ng ml}^{-1}$  for male adults.<sup>117</sup> Low testosterone levels can cause major issues such as undeveloped genitalia, skeletal and muscle development defects, and a loss of masculinity.<sup>118</sup> Total testosterone concentrations in saliva and serum were shown to be correlated ( $R = 0.70\text{--}0.87$ ); additionally, serum free and salivary free testosterone ( $R = 0.97$ ) were also shown to have statistically significant associations.<sup>119</sup> 3D disc-ring micro-electrode sensing platforms were used to detect testosterone electrochemically.<sup>120</sup> The free concentrations of steroid hormone in saliva have been determined to reflect the free, and unbound quantities in the blood.<sup>58,121,122</sup> The physiologically active portion of the overall concentration is considered the free fraction.<sup>123–125</sup> As a result, salivary progesterone and estrogen levels may be a better

measure of activity. Monitoring the concentrations of estrogen and progesterone in the saliva may be a way to track the menstrual cycle.

Saliva composition changes throughout the day and between people.<sup>126</sup> Saliva contents and concentrations are mostly reported using average compositions found in healthy people. Table II summarizes the components of genuine human saliva, as well as a comparison of the usual concentration, and ranges between saliva and other biological fluids. Saliva mainly contains sodium, potassium, calcium, thiocyanate, and phosphate. Low molecular weight chemical compounds including uric acid and lactate as well as essential hormones like cortisol, and high molecular weight chemical compounds including immunoglobulins and mucins can all be present in saliva. Natural saliva is rarely used in research since collecting and sterilizing a big quantity of spit is challenging. Additionally, saliva samples differ in composition and characteristics.<sup>127</sup> It fluctuates during the day and within each individual, as previously described,<sup>128</sup> a perfect reproduction of human saliva features is unachievable. To imitate real saliva, the mixture was created with similar components and properties, called synthetic artificial saliva. Synthetic saliva should work similarly to real saliva in the organism or with the test material in biosensing. According to Leung et al.,<sup>128</sup> who compiled numerous formulas published between 1931 and 1997, there are several synthetic saliva formulations in the literature. This article discusses five different synthetic saliva formulas that have been produced for various uses. Additionally, there are other recipes adapted for the study. As indicated in Table III, some of these formulations contain just inorganic compounds that are employed in vitro research,<sup>129–133</sup> whereas others contain both organic and inorganic compounds and proteins.<sup>127,134</sup> Only inorganic compositions that are comparable to an average composition of human saliva are used in the AFNOR, Fusayama–Meyer, and SAGF recipes. The mixture was also selected based on the similarity of testing results from manufactured saliva and genuine human saliva.<sup>129</sup> The presented recipes were used in the research of materials' electrochemical behavior and resistance to corrosion in dental applications.<sup>129–133</sup> Saliva viscosity is caused by organic material and some proteins, which may affect the diffusion of other solutes, and hence some reaction rates. Note that the viscosity of human entire saliva is approximately 1.30 relative to distilled water.<sup>135</sup> The viscosity of saliva samples that have been centrifuged and filtrated to eliminate viscous components approaches that of distilled water. Due to the practical difficulty of finding adequate materials, there is no attempt to imitate the viscosity of real saliva while making artificial saliva for electrochemical and chemical studies. As a result, most electrochemical investigations used exclusively inorganic artificial saliva formulations. For the use of in vitro models to investigate dental biofilms, organic materials and proteins are required to imitate the medium as nearly as feasible. For example, in Shellis's cultural study of dental plaque,<sup>127</sup> the separation of salivary glycoproteins from bovine submandibular glands was the initial step in an artificial saliva preparation.

Furthermore, saliva can reflect the mental state and the saliva-based diagnosis can help in the clinical diagnosis.<sup>154</sup> Saliva has also played a key role in the COVID-19 pandemic. In 2020, the FDA has approved the saliva test as the emergency test for the SARS-CoV-2 infection<sup>155</sup> because it is comparable with the standard nasopharyngeal swabs.<sup>6,154</sup> In addition, the saliva-based test kit is a rapid and less invasive method by targeting bio-analytes rather than the pathogen which can control COVID-19 spread.<sup>136</sup>

### Advances in Lab-in-a-Mouth Sensors and Point-of-Care Sensors for Salivary Samples

**Lab-in-a-mouth sensors for monitoring pressure and other vital parameters.**—Fiber Bragg Gratings (FBG), internal sensors involving the optical fiber core. It was utilized as a sensor placed in the flexible dental device to investigate the activity of inducing and monitoring muscular fatigue in a patient for the treatment of

bruxism. The device with the FBG embedded sensor inside the initial molar tooth was fabricated and used for in vivo tests (Fig. 4A). The upper left first molar deformations during various movements monitored by the FBG sensor were demonstrated to determine and help understand the muscle fatigue process. The difference of each bite force pattern is examined at each level of the produced fatigue. This study showed the feasibility of comparing the sensitivity coefficients for the exhaustion and fatigue phases as 1.37 and 2.54 N s<sup>-1</sup>, respectively. In addition to the compared coefficients, the different bite force pattern was correlated to the facial thermal profile. The understanding of these characteristics could facilitate an examination and treatment of patients with bruxism symptoms.<sup>156</sup>

Additionally, *cavitas* devices for exercise were also developed. In Fig. 4B, the mouthguard sensor—including a double layer of 2-mm ethylene vinyl acetate (EVA) mouthguard materials and two force sensors (i.e., piezoresistive force sensors with a measurable force range from 0 to 111 N) on both sides of the maxillary first molars—was fabricated for monitoring teeth clenching during exercise. This example is significant for applications in sports and health. The output voltage of the force sensor in mouthguard materials increased linearly up to a load of 70 N. The developed sensor was successfully characterized by four simple types of dental-occlusion tests including teeth clenching, teeth tapping, jaw movement, and teeth grinding tests. The mouthguard sensor exhibited the trends of an occlusal analysis that confirmed those obtained results from an electromyogram (EMG) and adequate temporal resolution for the timing of teeth clenching. In the jaw movement test, the sensor outputs relied on the sensor position when the jaw moved. The teeth-grinding test at the mouthguard sensor also agreed with the measured video-motion results. Furthermore, the usefulness of the mouthguard sensor was confirmed by exercise tolerance analysis using an electromagnetically braked cycle ergometer under practicable sports conditions. The developed wearable mouthguard sensing device was found to be a beneficial tool for monitoring teeth clenching behaviors during the exercise that can further contribute to understanding and explaining the correlation between these tendencies and sports performance.<sup>157</sup>

The mouthguard-based devices were also applied for measuring head impacts in sports (e.g., American football). The number, frequency, and severity of head impacts encountered by athletes during play are critical to be quantified for evaluating player safety interventions. The developers applied the head impact sensing system—comprising of a custom-fit mouthguard sensor instrumented with flexible electronics (i.e., charging coil, a microcontroller unit (MCU), linear and angular accelerometers, and battery) and the developed machine learning model—to filter head impacts from spurious activities gathered during football games (Fig. 4C). A wide range of machine learning model algorithms and predictive characteristics based on six-degree-of-freedom (6DOF) kinetic data at a mouthguard sensor worn by—players during football matches were evaluated. This developed mouthguard sensor provided a direct measurement of angular acceleration, unlike the existing wearable systems that compute angular acceleration through either an array of linear accelerometers or differentiation of angular rate. Different machine learning models were instructed and evaluated their capability to distinguish between head impacts and spurious signals by using the video dataset collected by the sensor during games in 2018–2019. The overall precision and accuracy of the head impact detection system were 98.3% and 81.6%, respectively. (81.6% of video-confirmed head impacts by the sensor alone and 98.3% precision and 81.6% recall by the machine learning classifier). This combination of mouthguard sensor and machine learning-based head impact detection system offers a broad range of important applications such as equipment improvements, player education, and rule changes.<sup>158</sup> As the use of wearable sensors and neurological tests for clinical studies on high-risk populations (e.g., contact sports players and brain injury) rapidly grows, the platform that can share these data between relevant institutions is thus extremely required to



**Table II. Components of genuine human saliva, as well as a comparison of the usual concentration, ranges between saliva and other biological fluids.**

Real saliva composition	Health conditions	Normal range		References
		Saliva (mmol l <sup>-1</sup> )	Other biological fluids (mmol l <sup>-1</sup> )	
Na <sup>+</sup>	Nausea (one of the symptoms of uremia due to CKD), Cystic fibrosis, Hypertension	20–80	Plasma 145	6, 136, 137
K <sup>+</sup>	Muscle activity, Chronic kidney disease (CKD)	20	4	
Ca <sup>2+</sup>	Homeostasis, Malignant parotid gland cancer	1–4	2.2	
Cl <sup>-</sup>	Dehydration, Cystic fibrosis	30–100	120	
HCO <sub>3</sub> <sup>-</sup>	Chronic kidney disease	15–80	25	
Phosphate	Malignant parotid gland cancer	4	1.2	
Mg <sup>2+</sup>	Malignant parotid gland cancer	0.2	1.2	
SCN <sup>-</sup>	Oral cavity inflammation	2	< 0.2	
Uric acid	Gout, renal disease, oral cavity cancer, hypertension, obesity and metabolic syndrome, type 2 diabetes	3.38 ± 0.21 mg dl <sup>-1</sup>	Serum 6.31 ± 0.24 mg dl <sup>-1</sup>	6, 136, 138, 139
		217.2 ± 110.3 mol l <sup>-1</sup>	—	
		0.1–7.5 mg dl <sup>-1</sup>	—	
Bilirubin	Anemia, coronary artery infections, hepatic dysfunction, biliary duct, brain damage, and death	0.5–5.0 μmol l <sup>-1</sup>	Serum 0.2–1.2 mg dl <sup>-1</sup>	6, 81, 82, 137
Creatinine	An indicator of renal dysfunction such as chronic kidney disease (CKD)	0.12 ± 0.06 mg dl <sup>-1</sup>	Serum 0.89 ± 0.17 mg dl <sup>-1</sup>	6, 84, 137, 139, 140
		0.05–0.2 mg dl <sup>-1</sup>	Serum 0.6–1.5 mg dl <sup>-1</sup>	
Glucose	Diabetes mellitus	91.3 ± 10.1 mg dl <sup>-1</sup>	Plasma 80–120 mg dl <sup>-1</sup>	6, 136, 137, 139
		4–13 mg dl <sup>-1</sup>	—	
Cholesterol	Diabetes mellitus, cardiovascular disease	0.02–5.46 μmol l <sup>-1</sup>	Serum < 5 mmol l <sup>-1</sup>	6, 137, 139, 141
Lactate	Sepsis, hypoxia, metabolic disorders, and sports medicine	0.1–1.8	Serum 0.5–1.0	6, 142
		0.1–2.5	—	
α-Amylase	Stress biomarker	19–308 U ml <sup>-1</sup>	Serum 0.05–0.125 U ml <sup>-1</sup>	136, 137, 139
		93 ± 62 U ml <sup>-1</sup>	—	
		2.64 ± 1.8 mg dl <sup>-1</sup>	—	
Secretory-IgA	Periodontal disease	80–717 mg dl <sup>-1</sup>	Serum 70–400 mg dl <sup>-1</sup>	6, 136, 137, 143
		124.3–333.5 μg dl <sup>-1</sup>	—	
Mucins group	Oral cavity from an array of diseases, fungal infection, a viral infection of T cells, and surface attachment of cavity-forming bacteria	MUC5B: 2.4 ± 1.7 U ml <sup>-1</sup>	Serum 9.9 ± 0.8 ng ml <sup>-1</sup>	6, 144,145
		1.19 ± 0.17 mg ml <sup>-1</sup>	—	
Total proteins	Diabetes, cardiovascular disease, cancer	7.1–223.2 mg dl <sup>-1</sup>	Serum 6–8 g dl <sup>-1</sup>	6, 136, 137, 146, 147
		0.9 ± 0.2 mg ml <sup>-1</sup>	—	
Lysozyme	—	3–50 μg ml <sup>-1</sup>	Serum 7.4 ± 1.8 mg ml <sup>-1</sup>	6, 136, 137
		59.7–1062.3 μg ml <sup>-1</sup>	Serum 4–9 μg ml <sup>-1</sup>	
Albumin	—	0.2 ± 0.1 mg ml <sup>-1</sup>	Serum 3.5–5.5 g dl <sup>-1</sup>	
Cortisol	Psychological disorders and adrenal hormone function	3.5–27.0 mg dl <sup>-1</sup>	Serum 2–25 mg dl <sup>-1</sup>	6, 139
Testosterone	Sexual dysfunction, loss of vigor, poor physical performance, fractures	32–55 pg ml <sup>-1</sup>	Serum 320–600 ng dl <sup>-1</sup>	6, 148
Progesterone	Autoimmune diseases, such as Sjögren's syndrome, systemic lupus erythematosus, rheumatoid arthritis, multiple sclerosis, and autoimmune thyroiditis	Luteal phase 436 ± 34 pmol l <sup>-1</sup>	Serum Male: < 1 ng ml <sup>-1</sup>	6, 149
		Follicular phase 22.1 ± 2.7 pmol l <sup>-1</sup>	Serum Female: 15–60 ng ml <sup>-1</sup>	
Estrogen (Estradiol)		Luteal phase 20.6 ± 0.4 pmol l <sup>-1</sup>	Serum Male: 15–60 pg ml <sup>-1</sup>	
		—	Serum Female: 15–3700 pg ml <sup>-1</sup>	

Table III. Compositions of artificial saliva recipes.

Artificial saliva compositions	Concentration (mM)					
	AFNOR <sup>130,133</sup>	Fusayama-Meyer <sup>129</sup>	SAGF <sup>131,132</sup>	Klimek <sup>134</sup>	Shellis <sup>127</sup>	Bellagambi, Francesca G <sup>150-153</sup>
	Inorganic compounds					
NaCl	114.7	6.84	2.22	9.98		6.84
KCl	16.1	5.37	12.88	17.04	15.56	5.37
Na <sub>2</sub> HPO <sub>4</sub>	1.83	—	—	2.4	2.64	4.22
KH <sub>2</sub> PO <sub>4</sub>	1.47	—	4.85	2.42	2.57	—
NaHCO <sub>3</sub>	4.17	1.19	7.5	—	6.43	3.57
KSCN	3.4	—	1.96	1.97	2.36	—
				(NaSCN)		
CaCl <sub>2</sub> ·2H <sub>2</sub> O	—	4.69	1.56	1.16	1.43	5.4
Na <sub>2</sub> S·9H <sub>2</sub> O	—	0.02	—	—	—	—
Urea	—	16.65	3.33	3.33	2.83	66.6
NaH <sub>2</sub> PO <sub>4</sub> ·H <sub>2</sub> O	—	5	—	—	—	—
NH <sub>4</sub> Cl	—	—	—	2.99	4.36	—
Na <sub>2</sub> SO <sub>4</sub> ·10H <sub>2</sub> O	—	—	2.36	—	—	—
MgCl <sub>2</sub> ·6H <sub>2</sub> O	—	—	—	—	0.21	—
Sodium citrate	—	—	—	—	0.04	—
	Organic compounds (nonproteins and lipids)					
Ascorbic acid	—	—	—	0.01	—	—
Glucose	—	—	—	0.17	—	—
Uric acid	—	—	—	—	0.06	—
Creatinine	—	—	—	—	0.0009	—
Choline	—	—	—	—	0.12	—
Mixture of vitamins	—	—	—	—	0.8 mg l <sup>-1</sup>	—
	Protein/polypeptide compounds					
Mucin	—	—	—	2.70 g l <sup>-1 a)</sup>	—	—
Glycoprotein	—	—	—	—	2.5 g l <sup>-1</sup>	—
α-Amylase	—	—	—	—	300000	—
					Somogyi's unit l <sup>-1 a)</sup>	
Albumin	—	—	—	—	0.38 μM	—
Mixture of amino acids	—	—	—	—	41 mg l <sup>-1</sup>	—

a) Somogyi's unit l<sup>-1</sup> is a measure of the level of activity of α-amylase in blood serum. When working on a standard starch solution under established conditions, a Somogyi unit is defined as the amount of α-amylase necessary to create the equivalent of 1 mg of glucose.

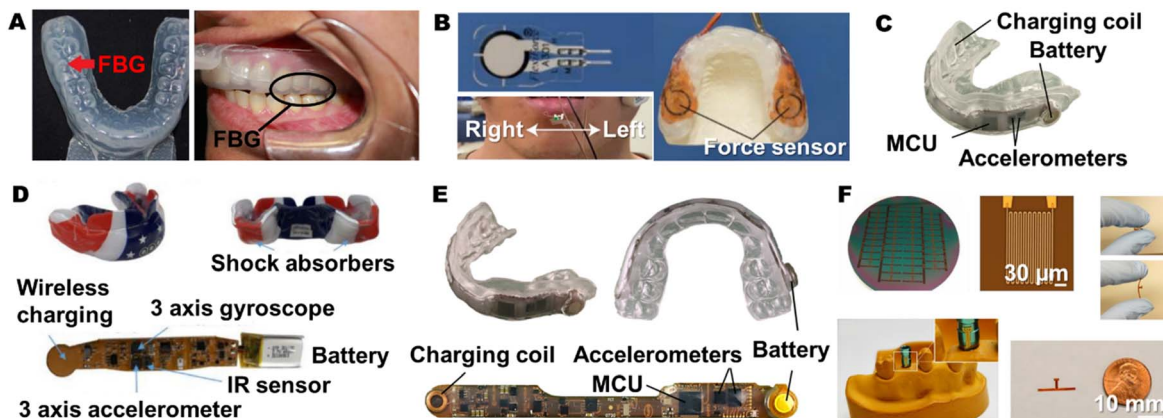


**Figure 4.** Sensors for monitoring pressure and vital parameters. (A) The FBG sensor integrated into the flexible occlusal device and the device at the bite position. Adapted under the terms and conditions of the CC-BY 4.0,<sup>156</sup> Copyright 2018, Nascimento et al., published by *Journal of Microwaves, Optoelectronics and Electromagnetic applications*. (B) The piezoresistive force sensor (top left), occlusal surface (right), and the grinding task for the subject (bottom left). Adapted under the terms and conditions of the CC-BY 4.0,<sup>157</sup> Copyright 2021, Kinjo et al., published by *Sensors*. (C) The mouthguard with accelerometer and flexible electronics. Adapted with permission,<sup>158</sup> Copyright 2020, Springer Nature. (D) The mouthguard for detecting head kinematics (top left), shock absorbers put at the molars for minimizing external disturbances (top right), and the sensor board at the incisors (bottom). Adapted under the terms and conditions of the CC-BY 4.0,<sup>159</sup> Copyright 2022, Domel et al., published by *Scientific Reports*. (E) Instrumented mouthpiece with flexible electronics (top left) and bottom (top right) views and an electronics board (bottom). Adapted with permission,<sup>160</sup> Copyright 2021, Springer Nature. (F) Temperature sensors (top left), a bright-field microscopic image of Pt resistor with overlapped Au interconnection lines (top middle), a highly flexible sensor (top right), a temperature sensor adhered around an abutment wing of the dental implant platform (bottom left), and small temperature sensor (bottom right). Adapted under the terms and conditions of the CC-BY 4.0,<sup>159</sup> Copyright 2020, Kim et al., published by *Sensors*.

promote the understanding of concussion mechanisms and help enhance the development of diagnostic tools. The Stanford instrumented mouthguard (MiG2.0) integrated the Federal Interagency Traumatic Brain Injury Research (FITBIR) informatics system and a deep learning impact detection algorithm (MiGNet) were developed as a new open-access platform for detecting and sharing mild traumatic brain injury (mTBI) data. An instrumented mouthguard (MiG2.0) that measured linear and angular head kinematics during an impact included the molded mouthguard and electronics embedded (Fig. 4D). The device measured 6DOF kinematics through a triaxial accelerometer and gyroscope. It was also detected when being worn using an infrared emitter-receiver IR pair that detected the light reflection. The sensory board was sealed with three ethylene vinyl acetate (EVA) material layers and placed at the incisors to distinguish sensors from extraneous disturbances. The communication between components happened through Bluetooth. The shock absorbers were put at the molars to reduce mandible disturbances from chewing, biting, and talking while wearing the device on the teeth. The BiteMac application was developed to interface with the mouthguard (MiG2.0) so that the kinematic data collected at the device was accessed and shared to the FITBIR platform and the developed MiGNet based on a neural network model achieved 96% accuracy on an out-of-sample dataset of high school and collegiate football head impacts. This developed system opens the door for creating a standardized database for promoting the knowledge of concussion biomechanics.<sup>159</sup> In Fig. 4E, custom-fit instrumented mouthpieces with new and low-powered accelerometers were developed and validated for directly measuring linear and angular head acceleration over a broad range of impact conditions in American football. The device includes a flexible electronics board (i.e., battery-powered and hardware components for acquiring kinematics and storing the data in memory) embedded in thermoplastic materials that support wireless data transfer and charging. The sensing elements included low-powered linear and angular accelerometers which consume solely  $74 \mu\text{A}$  in total to detect 6DOF kinematics while other existing systems need  $883 \mu\text{A}$  or higher. The accuracy for detecting head kinematics was tested by employing two helmeted headforms instrumented with an instrumented mouthpiece and reference sensor instrumentation. Both obtained results were highly correlated. This developed mouthpiece consumes low power while retaining accuracy in a wide range of impact conditions.<sup>17</sup>

In addition to the mouthguard-based devices for sport applications, researchers developed a micro-temperature sensor for real-time monitoring of infectious diseases in dental implant systems (Fig. 4F). The small multi-channel temperature sensor (15-mm length and 1-mm width) that was efficiently adhered around a dental implant abutment wing was fabricated using a flexible film (i.e., polyimide) and noble metals (the platinum resistor as a sensing material and the gold interconnection lines as a conductive material and contact pad) through a microfabrication process. An additional chromium layer was created as an adhesion between the platinum or gold metals and the polyimide film. Each channel was contacted with a four-wire detection circuit where the current went via the external lines and the voltage drop could be monitored across the internal lines. As a result, the voltage measurement correlated resistance to the temperature with minimal effects from the gold resistance. Changes of resistance as the important signal at the developed sensor can be measured when temperature changes from 20 to 100 °C with a temperature coefficient of resistance (TCR) value of  $3.33 \times 10^{-3}$  per degree Celsius which covers the range for dental implant applications (20 to 50 °C). The resistance change to the temperature of the sensor is also independent of pH and diverse types of solution mediums (i.e., deionized water, phosphate buffer, and artificial saliva) owing to the chemically inactive behavior of the Pt resistor toward the solution. This work ends with addressing an additional consideration about system integration (i.e., wireless data transfer and power delivery) for future sensor development which will provide customized diagnosis.<sup>19</sup>

**Lab-in-a-mouth sensors and point-of-care (PoC) sensors for detecting salivary biomarkers: metabolites, electrolytes, and other chemicals.**—A typical biosensor consists of a receptor (enzyme, antibody, nucleic acid, cell, etc.), a transducer (electrochemical, optical, thermal, piezoelectric, etc.), and electronic equipment that produces measurable signals.<sup>161</sup> Among the various transducers, electrochemical and optical transducers were mainly utilized for salivary healthcare devices due to portability and sensitivity, which are covered in this review. An electrochemical transduction system is very commonly used for oral monitoring wearables along with PoC devices, based on its advantages, such as being easy to miniaturize, transmitting signals wirelessly, and fast response. However, the optical sensors are less desired for intraoral wearable

applications due to difficulties of miniaturization and packaging optical detector to oral wearable form-factor for in-mouth operation, while they are more desired for salivary PoC devices by utilizing smartphone camera as the portable and sensitive optical signal detector.<sup>24,30</sup>

Electrochemical signal transduction methods can vary depending on which type of signal is to read, such as amperometric, potentiometric, voltammetric, conductometric, and impedimetric. It can be determined by the types of occurring reactions on the biosensor's electrode surface between the bioreceptor and target analyte. We can simply classify, catalytic-based biosensors and affinity-based biosensors. The catalytic-based biosensors use enzymes as bioreceptors converting the target analyte (substrate) to another product by enzyme's catalytic reaction, and it usually measures the electrical signals of the product from which the targets react with the enzymes. For example, glucose amount can be measured by an amperometric method using glucose oxidase as a bioreceptor, glucose oxidase will selectively recognize glucose to produce gluconic acid and hydrogen peroxide, and electrochemical oxidation or reduction current of hydrogen peroxide is recorded upon the fixed potential is applied. And the resulting current response is proportional to the amount of glucose. This method can also be applied to other metabolites (e.g., lactate, uric acid, etc.) sensors using enzymes.<sup>17,19</sup> Affinity-based biosensors use bioreceptors such as an antibody, aptamer, and nucleic acid. In this case, the bioreceptors selectively bind to biomarkers such as specific chemicals, proteins, cells, or antigens, but do not have electrical activity nor convert the target analyte to other products, so they should add labels or use measurement solutions that contain redox probes. These sensors measure changes in charge transfer resistance of external redox probes or read changes in charge on surfaces as resistance or conductance when analytes are bound to the sensor.<sup>23,31,162</sup> For example, a sensor uses a peptide that selectively grabs the surface of a particular bacteria to bind gram-negative bacteria whose outer membrane is negatively charged and to measure bacteria by reading changes in resistance or conductance.<sup>16</sup> There is also a sensor that immobilizes angiotensin-converting enzyme-2 (ACE2), which selectively binds to spike protein of the COVID-19 virus, physically blocking the redox probe in an external solution from reaching the electrode surface when the COVID-19 virus binds to ACE2. The salivary ion level related to health conditions can also be measured using an electrochemical transducer.<sup>23,162</sup> For example, an ion-selective electrode (ISE) is made of a membrane usually containing ionophores, which can selectively recognize and grab ions (such as  $\text{Na}^+$ ,  $\text{K}^+$ , and  $\text{H}^+$ ) from saliva. As a result, it builds up the surface potential changes, we can simply translate it into ion concentration by operating the open-circuit potential technique.

In addition to electrochemical methods, optical methods mainly used in PoC sensors use chemiluminescence,<sup>163</sup> colorimetric,<sup>24</sup> fluorescence,<sup>30</sup> etc. Chemiluminescence-based biosensors emit light through a chemical reaction between a substrate (or product) and a luminophore. For example, there is a method of using a reaction between a recognition element labeled with horseradish peroxidase (HRP), hydrogen peroxide, and luminol.<sup>163</sup> When a target is present in the sample, the luminol becomes an excited state with HRP and hydrogen peroxide to emit light, and this is measured. In the case of fluorescence-based biosensors, fluorescent labels are bonded to bioreceptors which further bind to analytes. For example, RNA probes have a sequence to recognize RNA in the middle, a fluorescent material (Fluorescein phosphoramidite, FAM) that absorbs light of a specific wavelength and emits light of another wavelength at one end, and a quencher (black hole quencher, BHQ) that absorbs the wavelength emitted by the fluorescent material at the other end to utilize Förster resonance energy transfer (FRET). When there is no target in the sample, the distance between the quencher and the reporter is short in the probe, and thus fluorescence is not generated, but when the target is attached to the probe, the distance between the quencher and the reporter is increased. For PoC application, a colorimetric method is desired due to intuitive detection with naked eyes. Colorimetric is a method of measuring

the concentration of a chemical compound in a solution with the aid of a color reagent. In a general colorimetric method, the colorimetric dye changes or generates the color in the presence of the target analyte in the sample. It is applicable to both organic compounds and inorganic compounds and may be used with or without an enzymatic stage.<sup>163</sup> We found one example of the colorimetric salivary monitoring device, measuring glucose and nitrite on mouthguard form-factor. The biosensor can analyze glucose with an enzymatic stage and nitrite without an enzymatic stage. The sensor analyzes glucose using a bienzymatic system that uses glucose oxidase and horseradish peroxidase to produce a color compound through oxidative coupling. In addition, nitrite is quantified by measuring the azo dye produced in proportion to the amount of nitrite through Griess reaction. It is a good example of an optical salivary biosensor pointing out the differences of saliva monitoring devices between on-mouth operation and PoC devices along with the difficulties of optical devices being completely wearable. In detail, the mouthguard sensor is capable of saliva sampling inside the mouth while wearing, but the measurement mechanism is the same as the PoC because the device must be taken out of the mouth and the signal should be measured using a scanner or spectrophotometry outside the mouth.

*Metabolites.*—In the case of a specific disease, continuous measurement of biomarkers related to the disease is necessary to diagnose or examine the course of treatment. For example, in diabetic patients, continuous blood glucose, and continuous measurement in daily life can be used to control insulin doses or determine the dosage of blood glucose level regulators. Previous papers that revealed the correlation between metabolites and electrolyte concentrations in blood and saliva through in vitro experiments showed the potential of lab-in-a-mouth sensors and encouraged wearable salivary biomarker sensor exploitation, particularly in the form of mouthguards. Unlike one-time measurement equipment, continuous monitoring of saliva is difficult because of biofouling from salivary proteins. Pretreatments such as centrifugation or filtration are required to avoid such fouling issues for repetitive measurements. Mouthguard sensors have shown that lactate and uric acid, a type of metabolites, in saliva can be measured, but in both cases, they are electrochemically measured by following the hydrogen peroxide reduction signal (utilizing artificial peroxidase such as Prussian Blue).<sup>17,19</sup> Kim, Jayoung, et al.<sup>17</sup> addressed the difficulties of continuous measurement of actual saliva without any pretreatment through the introduction of an *o*-phenylene diamine layer in lactate mouthguard sensor (Fig. 5A). Salivary lactate level (up to 1.6 mM) corresponds well with blood lactate level (up to 17.3 mM) and shows one's physical stress and performance.<sup>73,74</sup> They demonstrated the selective and stable detection of a salivary lactate range of 0.1–1.0 mM using lactate oxidase, which is entrapped in poly(*o*-phenylenediamine) (PPD) layer during electropolymerization, in vitro for over 2 h of operation and electropolymerized *o*-phenylenediamine was utilized to protect against biofouling in whole human (untreated) saliva samples. Although the device can measure most of the normal saliva level range in raw saliva media, physical stress and performance related to lactate can be seen. This mouthguard device is the first example of a salivary biosensor on the wearable platform with continuous measurement. Then, Kim, Jayoung, et al.<sup>19</sup> combined wireless electronics to develop a wearable mouthguard salivary uric acid biosensor to solve the previous study's impossible telemetric measurement, which makes capable of continuous, noninvasive real-time monitoring of salivary uric acid levels possible as an alternative to blood uric acid levels related to hyperuricemia, and renal syndrome, among other conditions (Fig. 5B). As shown in Fig. 5B, the mouthguard sensor showed a stable response to salivary uric acid for over 4 h with negligible biofouling issues. This device could measure the concentration of uric acid in saliva, in the normal range (100–250  $\mu\text{M}$ ) and up to 600  $\mu\text{M}$ , demonstrating that it can be used to diagnose and monitor the therapeutic process of gout, asymptomatic hyperuricemia, by testing saliva samples from individuals with



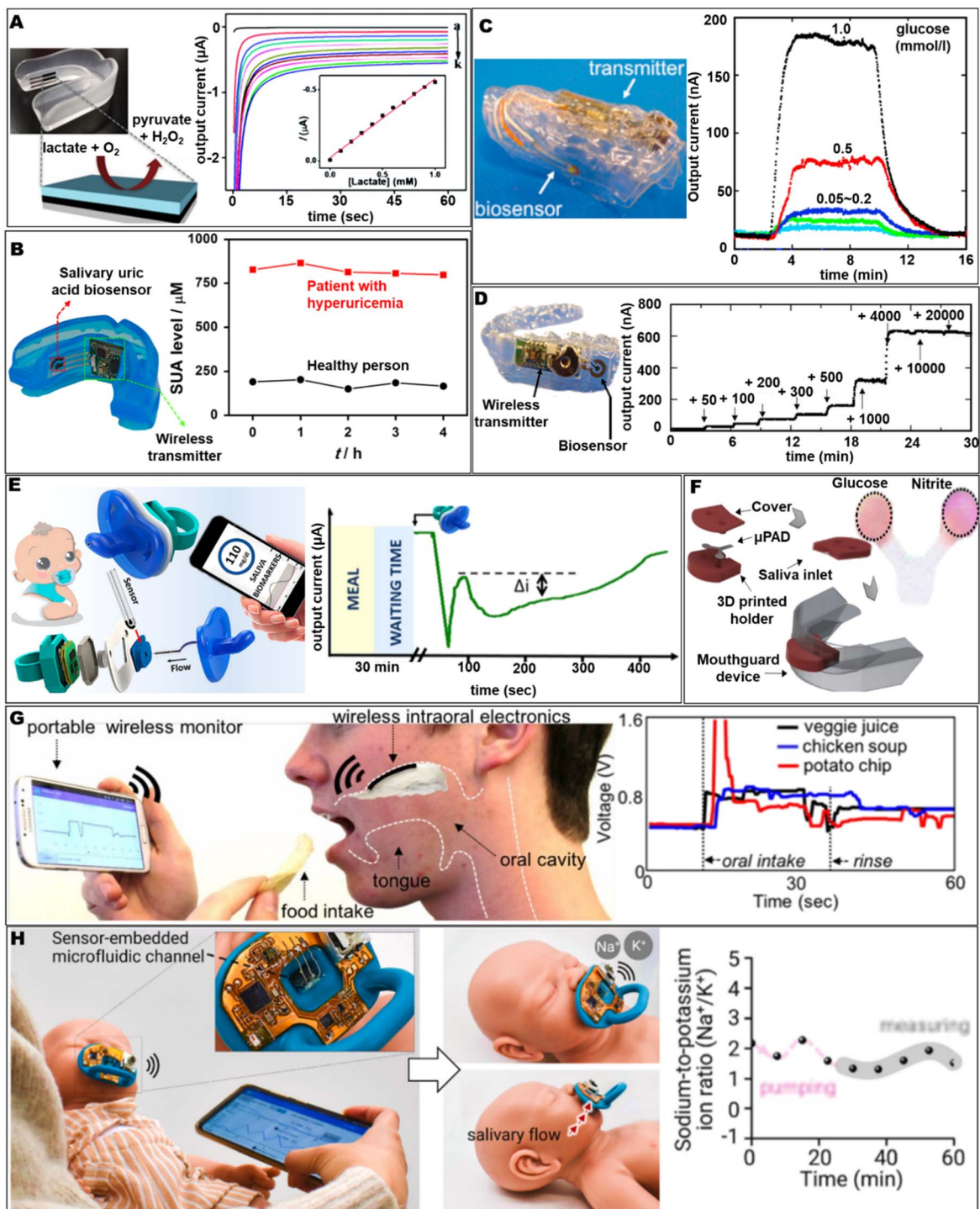


**Figure 5.** Sensors for monitoring metabolites and other chemicals. (A) photograph of the mouthguard lactate sensor & schematic illustration of the sensor for lactate (left), and the response obtained for increasing lactate concentration (right). Adapted with permission,<sup>17</sup> Copyright 2014, the Royal Society of Chemistry. (B) photograph of the mouthguard uric acid sensor (left), Monitoring of the salivary uric acid level of healthy and hyperuricemia patient (right). Adapted with permission,<sup>19</sup> Copyright 2015, Elsevier. (C) Image of custom-fit mouthguard glucose sensor (left), the response of the glucose sensor in the phantom jaw system (right). Adapted with permission,<sup>21</sup> Copyright 2016, Elsevier. (D) Photograph of mouthguard glucose device (left), the response of glucose in sample saliva (right). Adapted with permission,<sup>26</sup> Copyright 2020, American Chemical Society. (E) Concept of pacifier glucose sensor (left), schematic amperometry response of glucose monitoring (right). Adapted with permission,<sup>77</sup> Copyright 2019, American Chemical Society. (F) Scheme of the  $\mu$ PAD in 3D-printed mouthguard (left), the colorimetric response of glucose and nitrite (right), Adapted with permission,<sup>24</sup> Copyright 2019, Springer Nature. (G) Concept of the intraoral sodium intake sensor (left), in vivo, the real-time response of different foods with a human subject (right). Adapted under the terms and conditions of the CC-BY 4.0,<sup>23</sup> Copyright 2018, Lee, Yongkuk, et al., published by *Proceedings of the National Academy of Sciences*. (H) Overview of pacifier sensor for electrolyte monitoring (left), Real-time and continuous monitoring response of sodium and potassium ion levels for an hour (right). Adapted with permission,<sup>162</sup> Copyright 2022, Elsevier.

hyperuricemia. The first generation of a mouthguard was developed for fitness applications by measuring salivary lactate; the second generation was developed for clinical monitoring by detecting salivary uric acid.

Diabetes, a type of chronic disease without a definite cure, is diagnosed according to the blood glucose level, and patients with diabetes are recommended to manage their blood glucose levels below a certain level to prevent various complications caused by diabetes. However, to measure blood glucose levels, samples must be collected too often through invasive methods, which causes inconvenience to patients. It has been reported that there is a correlation between blood and salivary glucose.<sup>65</sup> Therefore, sensors have been developed to measure glucose in saliva. Arakawa, Takahiro et al.<sup>26,76</sup> measured the oxidation of hydrogen peroxide generated by the reaction of glucose oxidase using amperometry on an intraoral wearable platform. Intraoral biosensing devices have been further developed into smaller *cavitas*-type device that fits over the user's teeth for monitoring salivary glucose and contributes to the evolution of glucose sensors from invasive to noninvasive methods.<sup>76</sup> (Fig. 5C) Glucose oxidase membrane modified electrode was formed on the polyethylene terephthalate glycol surface of the mouthguard to which the wireless receiver was combined. The glucose sensor provided real-time continuous wireless monitoring of glucose in artificial saliva containing ions and proteins from 0.05–1.0 mM in vitro with a phantom jaw mimicking the human oral cavity, which corresponds to the normal glucose concentrations in human saliva of 50–100  $\mu\text{M}$ .<sup>164</sup> However, it was assessed by setting the flow rate to 0.5 ml min<sup>-1</sup> rather than using a system that replicated the real flow of saliva in the human oral cavity, and this device cannot be used for continuous saliva monitoring. To prevent biofouling that occurs during in vivo monitoring of human saliva in the previous study of the same group, Arakawa, Takahiro, et al.<sup>26</sup> have further continued the development of mouthguard glucose sensor by demonstrating that a cellulose acetate membrane as an interference rejection membrane on a mouthguard glucose sensor makes it possible to monitor salivary glucose successfully in vivo without any pretreatment of human saliva (Fig. 5D). The sensor device<sup>26</sup> was able to operate in vivo and could measure the concentration of 0.03–10.03 mM glucose. In another case, a wearable glucose sensor in the form of a pacifier on which the baby's mouth motions mechanically pump saliva to create a unilateral flow from the mouth to the electrochemical chamber has also been reported (Fig. 5E).<sup>77</sup> Unlike the aforementioned sensors, this baby device was developed in the form of a pacifier to separate the electrochemical chamber from the oral cavity, preventing leakage of chemicals from electrochemical sensors. The device can continuously on-body monitor glucose in saliva and a good correlation between the signal obtained with this pacifier device and the commonly used glucometer-fingertip blood signal of glucose in saliva was shown. Electrochemical detection of the hydrogen peroxide reduction, catalyst reaction of Prussian blue, after converting to hydrogen peroxide using glucose oxidase measured by amperometry. A Microfluidic paper-based device ( $\mu\text{PAD}$ ) was also integrated into the mouthguard platform, measuring salivary glucose and nitrite in a single device (Fig. 5F).<sup>24</sup> It showed a linear sensing response behavior ( $R^2 = 0.994$ ) for glucose and nitrite in concentration ranges of 0.027 to 2.0 mM and 0.007 to 0.4 mM, respectively in artificial saliva. Nitrite, a periodontitis biomarker, is detected by the Griess reaction, which causes Griess reagent to change to pink-red azo dye. In the presence of a chromogenic substance, glucose is detected using a bienzymatic assay including glucose oxidase and horseradish peroxidase. When this mouthguard sensor operates in actual saliva samples using the corresponding colorimetric instrument, there was no difference in reliability by 95% compared to the reference spectrophotometric measurement. The sensors were further tested with healthy, diabetic, and periodontitis patients. The sensors can measure normal glucose concentration in a range of 0.04–0.34 mM,<sup>165–167</sup> diabetic glucose concentration in a range of 0.55–1.39 mM,<sup>165,167</sup> and nitrite concentration in a range under 200  $\mu\text{M}$  nitrite (normal people without periodontitis).<sup>168</sup> The colorimetric detection has a limit in

quantification with naked eyes, rather it requires an additional read-out device for accurate quantification. The current version, detection by office scanner and spectrophotometer, did not allow color measurement in-mouth without taking them out. Therefore, it may be used as a method of diagnosing, but it is not suitable as a method of monitoring the health status of the wearer practically.

In the case of diabetes, salivary glands affected by changes in hormonal and neural balance increase salivary glucose levels. The development of equipment using this monitoring of salivary glucose levels as an alternative indicator to the level of blood glucose might offer a comfortable screening route for diabetes patients.<sup>167,169–173</sup>

It has the advantage of measuring glucose in saliva rather than glucose in the blood. Therefore, considerable efforts are being made to develop wearable salivary glucose biosensors, but limitations still exist. According to Soni et al., the correlation between blood glucose concentrations and saliva glucose concentrations in healthy persons is only  $R = 0.64$ .<sup>75</sup> Thus, further research is needed before salivary glucose levels can be used to screen for diabetes or monitor it using intraoral biosensing platforms. Although it has been discovered that blood glucose levels and saliva glucose levels are related to diabetics, a problem can be the contamination by external factors even in the case of diabetics. The possibility of gum bleeding, which can make false signals through saliva contamination, should also be considered. Several proteins present in saliva, as well as food debris, cause sudden biofouling of devices through nonspecific adsorption, which is one of the biggest challenges in the practical application of wearable biosensors. If the aforementioned saliva contamination problem is solved, diabetes can monitor salivary glucose continuously, instead of using blood glucose. However, further studies must be done to replace invasive methods used to diagnose and manage diabetes with large size of clinical trials considering various severities of diabetes, and differences between individuals.

*Electrolytes and other chemicals.*—In addition to the metabolites, electrolytes, and other chemical/biological biomarkers in saliva have also been measured using intraoral biosensors.<sup>23,162,174</sup> An intraoral biosensor has been developed that can measure the amount of sodium in food consumed during food intake (Fig. 5G).<sup>23</sup> Ultrathin stretchable electronics and tiny sensors are used in this intraoral device. The device has been tested on humans, demonstrating its capability to monitor sodium consumption in real-time, which is important for managing high blood pressure (hypertension). The study demonstrated toxicity for in vivo studies. However, the chemical sensing layer's toxicity was not assessed, so feasible intraoral applications would require further inspection of biocompatible recognition layer. Additionally, further work is needed to measure sodium uptake during a wider range of food and beverage. Surface fouling and contamination caused by additional saliva ingredients and food debris, respectively, should be tested. In 2022, the same group developed a device that could continuously measure salivary sodium and potassium in real-time by integrating microfluidic channels, flexible circuits, and ion-selective sensors into a commercial pacifier (Fig. 5H).<sup>162</sup> This sensor showed that sodium and potassium concentrations in saliva could be continuously measured in vivo, and the measured concentration ranges of sodium and potassium in saliva were 5.7–9.1 mM (sodium) and 4.2–5.2 mM (potassium), respectively. The device can measure the ratio of sodium to potassium by measuring the sodium and potassium respectively, the ratio is known that the ratio of sodium to potassium in the saliva is related to various health problems such as hypertension, cardiovascular disease, aldosteronism, and chronic kidney disease.<sup>90,175–177</sup> Therefore, it has been shown that the device can monitor electrolytes in a non-invasive manner in newborns and that it can be used to diagnose cardiovascular diseases. The development of artificial tongues has also been reported as an intraoral sensor that measures chemicals involved in the tasting. Yeom, Jeonghee, et al.<sup>174</sup> reported that saliva-like chemiresistive ionic hydrogel immobilized flexible substrate mimicking the mechanism by which the human tongue recognizes astringency can be used as an artificial

tongue. When the sensing material is exposed to an astringent substance (tannic acid), hydrophobic structures create inside the microporous hydrogel and transform it into a micro/nanoporous structure with increased ionic conductivity. This human tongue-like sensor for tannic acid has been proven to measure a wide range (0.0005 to 1 wt%) with high sensitivity ( $0.292 \text{ wt}\%^{-1}$ ) and fast response time ( $\sim 10 \text{ s}$ ). This sensor can measure the degree of astringency in drinks and fruits using a simple detection method, however, it does not include a system that can obtain, process, and transmit measured data wirelessly. In addition, it should be considered whether it works selectively for hydrophobic compounds such as cholesterol found in foods commonly consumed as sensors based on hydrophobic aggregation.

Future work on practical in-mouth applications will necessitate rigorous validation tests in comparison to blood, as well as a thorough review of safety concerns such as biocompatibility, possible toxicity, sterilization, and operational stability. The use of biocompatible materials and effectively sealed devices including the supporting electronic interface and power supply is required to eliminate dangers associated with device contact with saliva particularly chemical leaching to the surrounding fluid. Sealing is also necessary for protecting the electronics' operation. In addition, the potential interferences from intraoral bleeding and food intake should also be considered for accurate monitoring. Changes in the biomarker concentrations and flow rate of saliva by daily stimulation, such as tongue sour stimulation, are also considered for the development of intra-oral biosensors. The continuous discovery of novel saliva biomarkers will aid in the expansion of saliva's diagnostic application scope. The introduction of multiplexed oral cavity biosensors could help with diagnostic capabilities.

**Lab-in-a-mouth sensors and on-demand sensors for detecting salivary drugs and their related toxic substances.**—The detection of salivary aldehydes is crucial for epidemiological studies and assessment of oral cancer risk and development. In Fig. 6A, a three-dimensional microfluidic paper-based analytical device was successfully developed for noninvasive monitoring of total salivary aldehydes for the first time.<sup>178</sup> This colorimetric paper-based sensor included two overlapping paper layers which contained fifteen circular detection zones (8 mm in diameter) impregnated with 3-methyl-2-benzothiazolinone hydrazone (MBTH) at the first layers and fifteen circular reagent zones (4 mm in diameter) at the second layer. Iron (III) chloride was added to reagent zones after adding the sample to the detection zones. All hydrophilic zones were defined using the wax printing technique. The colorimetric measurement was based on a two-step reaction between the target aldehydes, MBTH, and iron (III) to form a blue-colored formazan dye. The formed color intensity within each detection zone was measured using Image J software. The developed colorimetric microfluidic paper-based device provided a detectable range from 20.4 to 114.0  $\mu\text{M}$  of salivary acetaldehydes with the detection limit (LOD) of 6.1  $\mu\text{M}$ , comparable to that of the standard gas chromatographic method (the LOD of 2.1  $\mu\text{M}$ ). The sensor was also validated with spectrophotometry as a reference method which showed no statistically significant difference at the 95% confidence level. This developed device, as an alternative to the conventional approaches (e.g., gas chromatography and high-performance liquid chromatography), further promoted routine assessment of oral cancer risk and development.

Miniaturizing the footprint of biosensing dielectric devices allows their widespread applicability for personalized healthcare. One remarkable example of this approach is the development of millimeter-scale trilayer radiofrequency (RF) sensors for measuring the oral cavity and food consumption (Fig. 6B). The developed sensor adopted a broadband coupled split-ring resonator (BC-SRR) consisting of biopolymer film and active sensing layers and the sensing interlayer was sandwiched between split-ring resonators. This geometrical construction permitted the measurement of changes in interlayer thickness, engineerable delays in antenna response via

controllable transport features of solutes into the interlayer, and improved sensitivity from the electric field intensity at the interlayer. Thickness and dielectric constants at the interlayer were changed when the interlayer swelled and absorbed the surrounding solvent. This led to changes in resonant frequency and amplitude of the sensor. The obtained signals at the sensing device were measured using an RF network analyzer linked to a reading coil. The in vivo sensing performance of the developed sensor was successfully demonstrated in common environments of the human mouth, including dry-mouth and liquid consumption (i.e., alcohol, apple juice, mouthwash, soup, and tap water) conditions. This miniaturized footprint that was convenient and adaptable to various environments extended the applicability of RF sensors for distributed and multiplexed sensing.<sup>179</sup> In Fig. 6C, the optical fiber-based platform was developed and integrated into a mouthguard as an intraoral optical sensor with the point or extended area sensing for the detection and assessment of wine intake. The intraoral optical sensor with point sensing or the point sensor included an LED source that applied light into a side-polished optical fiber. The LED was mounted on a flexible triangular sticker substrate adjacent to the bias resistance and pads for an external power supply (3 V). The LED and fiber footprints were drilled into the mouthguard. The LED was placed under the side-polished optical fiber to have the light applied over the polishing into the fiber core. The intraoral optical sensor with extended area sensing or the extended sensing area sensor included side and end emitting optical fibers, placed in parallel in a vertical coupler topology. Two parallel canals were drilled into the mouthguard to place the fibers in parallel. This placement was further parallel to the lingual slope and perpendicular to the dental arch, allowing the sensing surface to be exposed to saliva. The developed sensor displayed absorption spectra of wines that had specific differences with respect to the wine types, resulting in wine discrimination based on the spectral signature. The wine absorption spectra at the proposed sensor showed a fine resolution in both wavelength and amplitude domains to express wine color measurement in terms of brightness, chromaticity, and intensity. Hence, wine color characterization that gave information with respect to wine quality assessment was achieved using the proposed intraoral sensor. The proposed point or extended sensing area sensor was validated in the laboratory environment and proved to be applicable as an intraoral optical sensor for real-time intraoral sensing. The sensor selectivity was tested with grape-based soft and fizzy drinks. The obtained absorption spectrum differed from that of each wine, enabling wine discrimination from other drinks. This proposed intraoral fiber-optics sensor facilitates an integration into a mouthguard and holds the potential for real-time biomedical applications to in vivo measurement of food and beverage intake which will be able to predict the development of disease-signaling salivary biomarkers.<sup>183</sup> The development of a wearable electrochemical sensing device for simultaneous measurement of salivary  $\Delta^9$ -tetra-hydrocannabinol (THC) and alcohol was demonstrated to fulfill the need for rapid road-site testing of these substances for reducing risks of fatal accidents from their additive effect of abuse (Fig. 6D).<sup>28</sup> Another promising example of the developed method as a rapid assay for oral THC analysis within five minutes called "EPOCH" (express probe for onsite cannabis inhalation). This method achieved high sensitivity with a low LOD of  $0.17 \text{ ng ml}^{-1}$  THC that was compatible with the regulatory guideline ( $1 \text{ ng ml}^{-1}$ ).<sup>184</sup>

Thiocyanate ion is another significant biomarker for health-related problems. The first example of a detachable mouthguard sensor for fast monitoring of salivary thiocyanate ions was demonstrated (shown in Fig. 6E).<sup>184</sup> In addition, a fast and simple assay for in situ measurement of salivary thiocyanate ions was presented using a colorimetric paper-based sensing platform.<sup>180</sup> The developed paper-based sensing platform was based on a colored complexation reaction between iron (III) and thiocyanate under acidic conditions and a scanner was employed as a detection device for image analysis. The proposed method showed the LOD of thiocyanate as  $0.06 \text{ mM}$  at the optimal conditions and was also applied to measure



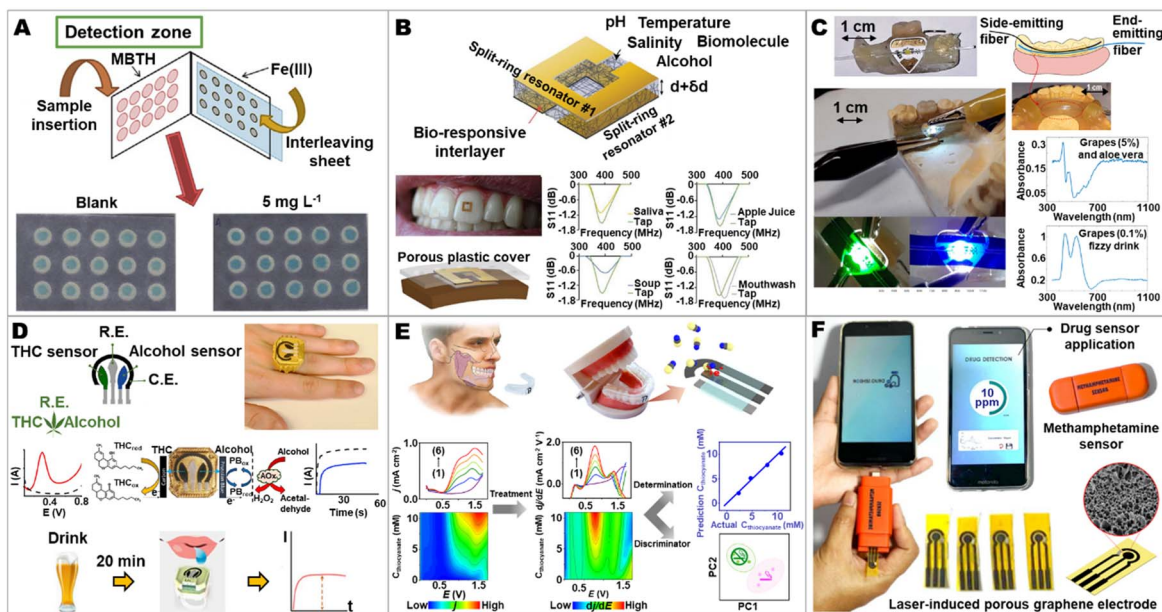


**Figure 6.** Sensors for detecting salivary drugs and related toxic substances. (A) The three-dimensional microfluidic paper-based analytical device for monitoring salivary aldehydes. Adapted with permission,<sup>178</sup> Copyright 2016, Elsevier. (B) Radiofrequency-trilayer sensors for detecting the oral cavity and food consumption; schematic of broad-side coupled split-ring resonators with an interlayer of silk film or responsive hydrogel (top), trilayer sensor attached to a human subject's tooth for in vivo analysis (bottom left), and the response on the subject to various liquids (bottom right). Adapted with permission,<sup>179</sup> Copyright 2018, John Wiley and Sons. (C) The intraoral optical sensor for identification and assessment of wine intake; the LED source and the optical fiber from the sensor structure integrated into a lateral mouthguard (top left), the side and the end emitting fibers deployed in parallel and integrated into a frontal mouthguard (top right), an experimental setup for the evaluation of the point intraoral sensor spectral attenuation measures (bottom left), and grape-based drink absorption spectra, acquired via the proposed intraoral point sensor (bottom right). Adapted under the terms and conditions of the CC-BY 4.0.<sup>28</sup> Copyright 2019, Faragó et al., published by *Sensors*. (D) The wearable electrochemical ring sensor for simultaneous monitoring of salivary  $\Delta^9$ -tetrahydrocannabinol (THC) and alcohol; sensor design for simultaneous monitoring of THC and alcohol (top-left), the image of a sensor platform incorporated with marijuana designed sensor for monitoring of THC-alcohol (top right), voltammograms of THC and alcohol measurements (middle row), and procedure used for gathering saliva samples after wine intake and measurement (bottom). Adapted with permission,<sup>180</sup> Copyright 2020, Elsevier. (E) The mouthguard device for detecting salivary thiocyanate ions and the developed analytical model for measuring thiocyanate concentrations. Adapted with permission,<sup>181</sup> Copyright 2021, Springer Nature. (F) The portable methamphetamine sensor. Adapted under the terms and conditions of the CC-BY 4.0,<sup>182</sup> Copyright 2021, Saisahas et al., published by *Nanomaterials*.

thiocyanate in human saliva samples. The average thiocyanate concentrations for nonsmokers and smokers were found in the ranges of 0.28–0.87 and 0.78–4.28 mM, respectively. This approach demonstrated the functionality of the developed paper-based sensing platform for monitoring salivary thiocyanate levels.<sup>35</sup>

Illegal drug use (e.g., methamphetamine) remains a global problem that threatens health and social harmony and stability. In Fig. 6F, laser-induced porous graphene (LI-PGr) electrode as an electrochemical sensor was fabricated for salivary methamphetamine analysis. The performance of the developed LI-PGr electrode as a portable electrochemical sensing device was investigated and successfully applied for monitoring methamphetamine (MA) on household surfaces and in salivary samples. The sensing device exhibited a wide linear range from 1.00 to 30.0  $\mu\text{g ml}^{-1}$  with a LOD of 0.31  $\mu\text{g ml}^{-1}$ , good precision, and reproducibility with a relative standard deviation of 2.50% ( $n = 10$ ), and excellent selectivity. This proposed method holds a great promise in forensic investigation and other relevant areas.<sup>29</sup>

**Lab-in-a-Mouth sensors and point-of-care sensors for detecting pathogens and infection status.**—Various samples that can be taken from the body are used to diagnose infections caused by pathogens or viruses,<sup>185</sup> but among them, sweat, saliva, and tears can be easily obtained in a noninvasive manner. Among them, saliva containing a variety of biomarkers produced from salivary glands, microorganisms, external substances, and permeating substances from blood has the advantage of being a sample for diagnosis.<sup>186</sup> The ability to quickly identify bacteria or viruses is a significant step toward more efficient and accurate treatment in clinical practice; yet, in both industrialized and developing countries, this remains a barrier, particularly when the pathogen is present in very low or undetectable

amounts. The detection methods for bacteria rely on culture, whereas the ones for viruses rely on PCR analysis. These methods need specific sample preparation procedures, which are time-intensive and expensive.<sup>187,188</sup> As a result, several studies have been conducted on low-cost, portable microfluidic devices,<sup>189</sup> the findings of which are described in this section (“Lab-in-a-mouth sensors and point-of-care sensors for detecting pathogens and infection status”). In 2012, Mannoor et al. developed one of the first saliva-based wearable devices to detect *H. pylori*.<sup>16</sup> (Fig. 7A) A simple transfer printing procedure is used to combine graphene monolayers with water-soluble silk fibroin films. Electrode patterns are printed on silk-graphene hybrid films, and this sensor is then transferred it onto a tooth's surface. Antimicrobial peptides self-assembled on the graphene surface enabled the recognition of certain bacteria even at the single-cell level. Due to its resonant coil, the device worked without on-board power or an external connection and was suitable for wireless monitoring. *H. pylori* was chosen as a target because it is one of the most common infections associated with duodenal ulcers. They demonstrated that the device could detect as little as 100 bacteria in a liter of material (and up to  $10^6$  cells), much below the bacterium's minimum infectious dose. They demonstrated that a battery-free, this device could be used to wirelessly monitor hazardous bacteria for several uses.

As the number of confirmed cases of SARS-CoV-2 infection, also known as COVID-19, has escalated fast, it has become an uncontrollable pandemic.<sup>191</sup> According to official WHO estimates, the pandemic has resulted in about 457,000,000 COVID-19 infections and 6,100,000 deaths (<https://covid19.who.int/>). This single-stranded positive-sense RNA virus from the coronavirus (CoVs) lineage is diagnosed by detecting viral RNA in respiratory specimens using real-time reverse transcription polymerase chain reaction



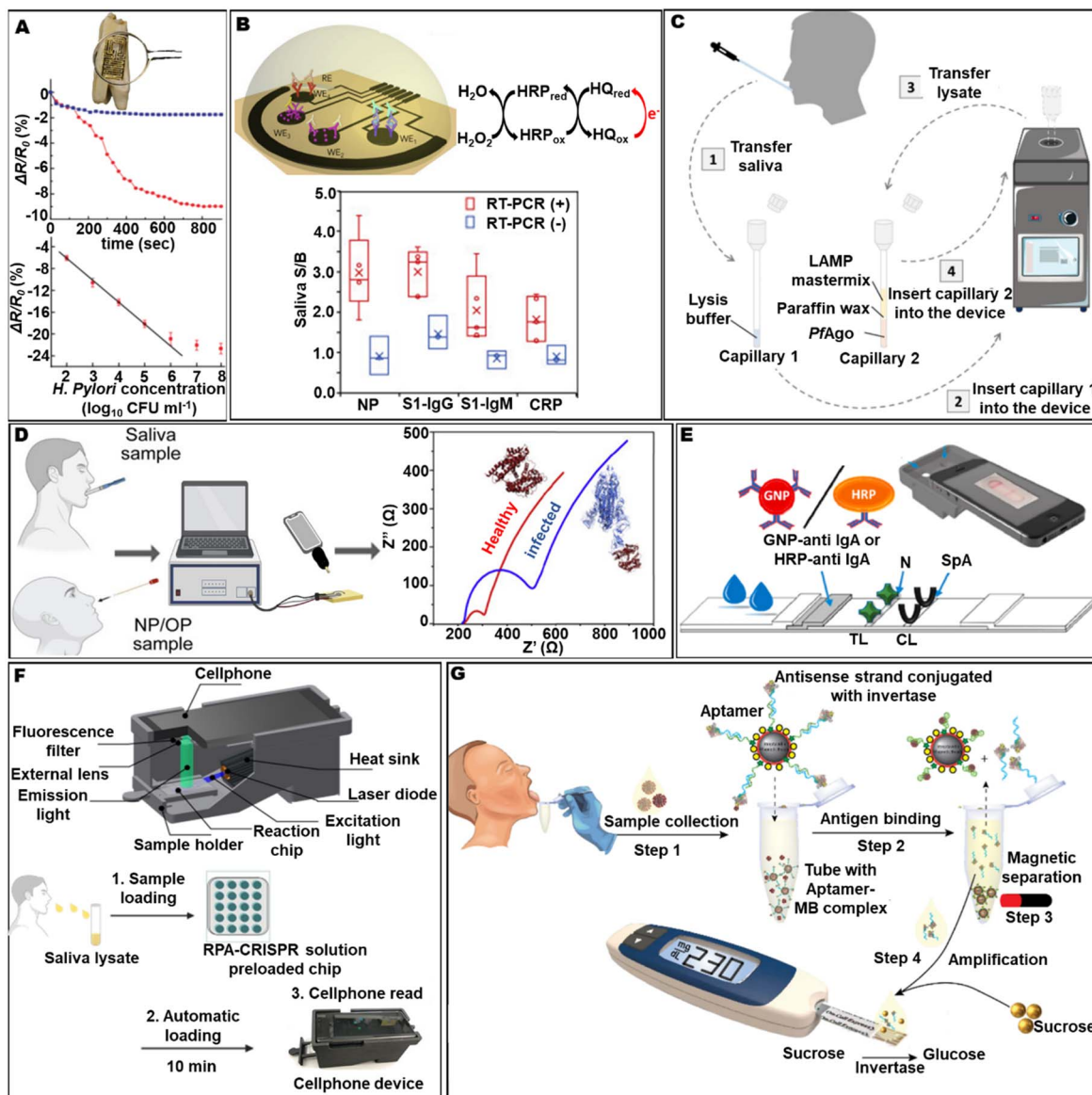


**Figure 7.** Examples of sensors for viruses and bacteria. (A) Photograph of the tooth enamel biosensor (top), response of *H. pylori* in human saliva (middle), response of *H. pylori* concentration (bottom). Adapted under the terms and conditions of the CC-BY 4.0,<sup>16</sup> Copyright 2011, Mannoor, Manu S., et al., published by *Nature communications*. (B) Schematic illustration of smartphone-based disposable COVID-19 sensor (top), the response of the sensor in confirmed COVID-19 positive and negative saliva samples (bottom). Adapted with permission,<sup>29</sup> Copyright 2020, Elsevier. (C) Overall schematic flow of SPOT device. Adapted under the terms and conditions of the CC-BY 4.0,<sup>190</sup> Copyright 2021, Xun, Guanhua, et al., published by *Nature communications*. (D) Graphical scheme of smartphone-based rapid COVID-19 sensor. Adapted with permission,<sup>31</sup> Copyright 2021, Elsevier. (E) Scheme of the strip to detect anti-SARS-CoV-2 IgA in a salivary sample and an image of smartphone-based optical immunosensor. Adapted with permission,<sup>163</sup> Copyright 2021, Elsevier. (F) The schematic flow of smartphone-read saliva test for COVID-19 (bottom), schematic of smartphone fluorescence reader (top). Adapted under the terms and conditions of the CC-BY 4.0,<sup>30</sup> Copyright 2021, Ning, Bo, et al., published by *Nature communications*. (G) Overview of an aptamer-based COVID-19 test strip. Adapted with permission,<sup>32</sup> Copyright 2021, Elsevier.

(PCR).<sup>192</sup> Saliva has recently been shown to be a feasible alternative to nasopharyngeal swabs, reducing patient suffering, the need for specialized medical personnel, and the risk of viral spread to the operator.<sup>145,193</sup> The use of saliva in the microfluidic PoC has also resulted in a reduction in diagnosis time, which is crucial in the present epidemic. The SARS-CoV-2 RapidPlex<sup>29</sup> is a multiplexed, wireless, portable electrochemical device for ultra-rapid COVID-19 detection. (Fig. 7B) It detects the inflammatory biomarker C-reactive protein as well as viral antigen nucleocapsid protein, immunoglobulin M (IgM), and immunoglobulin G (IgG) antibodies, using mass-producible laser-engraved graphene electrodes. This device is capable of ultrasensitive, selective, and rapid electrochemical detection in physiological ranges. Blood and saliva samples from COVID-19-positive and COVID-19-negative people. Based on the

findings of this study, multiplexed immunosensor technology may enable high-frequency at-home testing for COVID-19 wireless diagnosis and monitoring. Xun, Guanhua, et al.<sup>190</sup> have developed a quick scalable, and portable testing (SPOT) system for COVID-19 diagnosis that includes a fast, highly sensitive, and accurate assay as well as a battery-powered portable device. (Fig. 7C) The SPOT test involves one-pot reverse transcriptase-loop-mediated isothermal amplification (RT-LAMP) followed by argonaute protein from hyperthermophilic archaeon *Pyrococcus furiosus* (PfAgo) target sequence identification. In a multiplexed process, it can identify the N gene and E gene in SARS-CoV-2 virus spiked saliva samples in 30 min with a LOD of 0.44 copies  $\Gamma^{-1}$  and 1.09 copies  $\Gamma^{-1}$ , respectively. In addition, the SPOT system was used to analyze 104 clinical saliva samples, yielding 28/30 (93.3 percent sensitivity)

SARS-CoV-2 positive samples (100 percent sensitivity if LOD is taken into consideration) and 73/74 (98.6 percent specificity) SARS-CoV-2 negative samples. Many sensors that measure using cell-phones, the most accessible gadget, have recently been reported. According to Torres, Marcelo DT, et al., RAPID 1.0, a simple, portable, and miniaturized highly sensitive biosensor modified with human receptor angiotensin-converting enzyme-2 (ACE2), using electrochemical impedance spectroscopy, can recognize SARS-CoV-2 using 10  $\mu\text{l}$  of sample in 4 min.<sup>31</sup> (Figure 7D) For nasopharyngeal/oropharyngeal swab and saliva samples, RAPID's sensitivity and specificity are 85.3 percent and 100 percent, respectively. A device has been developed that monitors the COVID-19 virus using a method other than an electrochemical method and reads the signal on a smartphone. To correctly diagnose COVID-19 infection and its progression over time, immunoglobulins must be assessed quickly, sensitively, and noninvasively. Particularly, immunoglobulin A (IgA) in saliva and serum is necessary to complement assays that detect immunoglobulins G and M. Roda, Aldo, et al.<sup>163</sup> (Figure 7E) have developed a chemiluminescence/optical lateral flow immunoassay (LFIA) immunosensor for IgA in saliva and serum. A recombinant nucleocapsid antigen preferentially captures SARS-CoV-2 antibodies in patient material. A tagged anti-human IgA demonstrates the bound IgA fraction. Thanks to a combined colorimetric and chemiluminescence detection technique, measuring IgA to SARS-CoV-2 is both affordable and ultrasensitive. A simple smartphone camera-based technology measures the color signal produced by nanogold-labeled anti-human IgA. For sensitive chemiluminescence transduction, this device used a contact scanning handheld device with a cooled charge coupled device (CCD) to detect the optical signal resulting from the interaction of horseradish peroxidase-labeled anti-human IgA with an  $\text{H}_2\text{O}_2$ /luminol/enhancers substrate. The amount of salivary IgA in the study's participants ( $n = 4$ ) was shown to be related to the time from diagnosis and the severity of the illness. This IgA-LFIA immunosensor might be useful for noninvasively monitoring initial immune responses to COVID-19 and assessing the diagnostic/prognostic use of salivary IgA in huge screening to evaluate the efficacy of SARS-CoV-2 vaccines. A mobile, ultrasensitive saliva-based COVID-19 test was developed with a 15-min test time without RNA isolation or laboratory equipment (Fig. 7F).<sup>30</sup> In this test, the CRISPR-Cas12a is employed to amplify the viral amplicon signal, which is powered by the laser diode of smartphone-based fluorescence microscopy equipment. This device has a lower LOD ( $0.38 \text{ copies l}^{-1}$ ) than the RT-PCR standard test and reliably assessed viral load across a large linear range (1 to 105 copies/L). SARS-CoV-2 RNA levels assessed by CRISPR were comparable in the patient's saliva and nasal swabs, and viral loads assessed by RT-PCR and the smartphone-read CRISPR assay showed good correlation, indicating that this portable test may be employed for saliva-based PoC COVID-19 diagnosis. A device has been developed to diagnose COVID-19 by reading signals related to COVID-19 using a blood glucose meter (Fig. 7G).<sup>32</sup> Singh, Naveen K., et al. report an aptamer-based SARS-CoV-2 salivary antigen test that uses just low-cost reagents and an off-the-shelf glucometer. The test has constructed a glucometer as it is quantitative, easy to use, and the most ubiquitous piece of diagnostic equipment in the world, making it diagnose with current infrastructure. Many glucometers can connect to smartphones, allowing them to connect tracing apps, treatment professionals, and electronic health records. The developed assay detected SARS-CoV-2 in patient saliva with 100 percent sensitivity within 1 h throughout a range of viral loads—as measured by RT-qPCR—and distinguished diseased specimens from off-target antigens in noninfected controls with 100 percent specificity in clinical trials. This method provides a low-cost, quick, and accurate diagnosis for large-scale SARS-CoV-2 infection screening.

Tracking changes in the number of pathogens or viruses in the course of treatment can be helpful for dealing with symptoms and complications of the infectious disease. Importantly, detecting pathogens or viruses contaminated in the wearer's environment

can also decrease the spread of infectious diseases in a pandemic situation. Therefore, research on one-time PoC tools for diagnosis is also important, but wearable sensors (that can measure targeting pathogens or viruses in the environment or in patients' bodies) will be the future direction of the development. In addition, for infectious diseases that can spread even if they are asymptomatic, such as COVID-19, the wearable biosensor can prevent a person without symptoms from spreading to healthy others.

Biosensors for viral detection have been developed mainly in the form of PoC rather than in the form of an intraoral wearable. The advantage of intraoral wearable sensors is that it is possible to continuously measure while wearing them, so it can measure the daily fluctuation of salivary biomarkers. Thus, salivary sensors monitoring chronic diseases such as glucose or the need to maintain a certain level of health, such as ions, are reasonable to wear as wearable devices because they can help the wearer check their levels and maintain them in the normal range. However, in the case of highly contagious diseases with high mortality, such as severe acute respiratory syndrome (SARS), middle east respiratory syndrome (MERS), coronavirus disease-2019 (COVID-19), the confirmed patients are quarantined after diagnosis, so continuous monitoring of the wearer is not necessary to prevent the spread of the infectious disease, and a PoC system that can be detected without medical personnel is more needed. Of course, it would be nice to develop intraoral wearable biosensors that can diagnose diseases early in case of infection by continuously monitoring in daily life, but there are many technical hurdles (biocompatibility, toxicity, saliva contamination, etc.) in the process of moving from the PoC sensor to a wearable device that can be worn in the mouth. In addition, the diagnosis of infectious diseases is not quantitative analysis of the virus in the body, but only qualitative analysis. Thus, we prospect that saliva can be spit out once a day and diagnosed early enough with the PoC system, and there may be no need to develop it as a wearable device to overcome the aforementioned technical difficulties.

## Conclusions and Prospects

This article has described the anatomy and physiology of important cavities (focusing on the mouth) and highlighted recent progress in the rapid ongoing development of intraoral biosensing devices for various applications, such as sports, healthcare, medicine, and therapeutic drug management. Although considerable progress has already been made in lab-in-a-mouth sensors and PoC sensors for salivary samples, there are still several challenges and obstacles in practical real-world applications of *cavitas* mouth-guard-based sensing devices and artificial intelligence technologies for fully integrated systems.

The state-of-the-art integration technologies should be developed to realize miniaturized "all-in-one" biosensing devices, particularly a single mouthguard sensor with full functions.<sup>194</sup> Therefore, incorporating sensors, communication technologies, and power systems together is needed.<sup>195,196</sup> Many different types of electronics need to be integrated into a single device to include all essential functions, such as sensing system, signal, and data processing unit, power supply, wireless communication module, and cyber security system (Fig. 8).

The use of rigid or bulky analytical instruments such as a potentiostat (a commonly used tool for electrochemical detection methods) and a spectrometer, could limit the practical settings of wearable electronics devices or PoC sensors. The complicated manufacturing processes and materials still rely on rigid microelectronics components (e.g., resistors, conductors, and transistors). This represents another obstacle such as the lack of flexible electronics for integration onto soft substrates that would match the anatomy of the wearer.<sup>197</sup>

Advanced nanotechnology and emergent nanomaterials and composites have demonstrated a potential role in the development of portable, wearable, and miniaturized electronics sensing devices

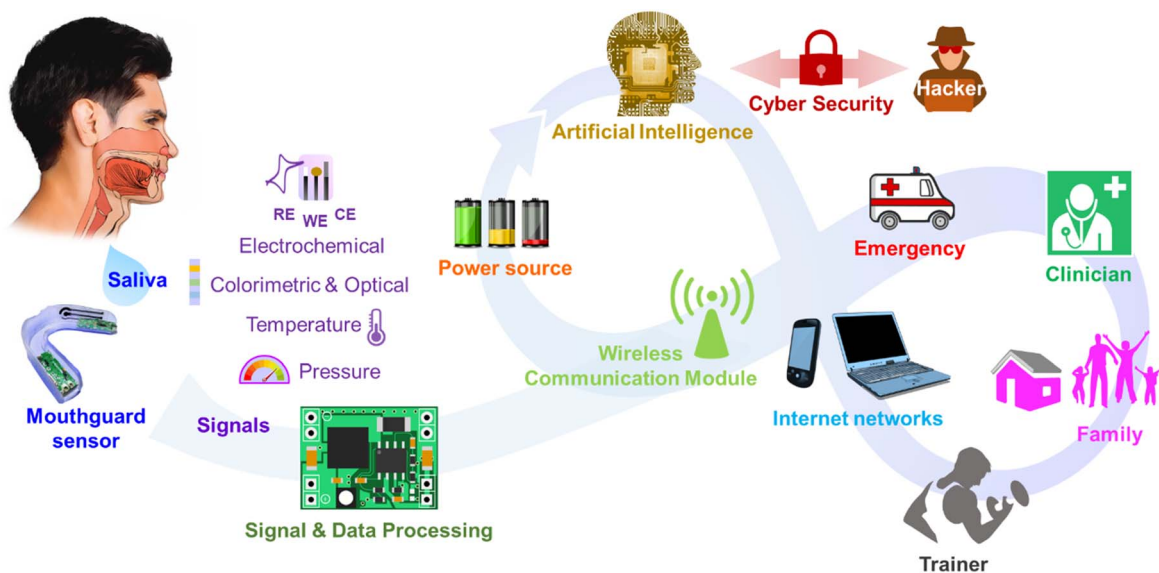


**Figure 8.** Conceptual diagram showing important building blocks of the next generation of smart health systems.

and designs with outstanding capabilities in many applications, ranging from quick diagnostic tools to modern biomedicine and healthcare.<sup>62,198–202</sup> For example, significant progress in the detection method for pharmaceutical quality control has been achieved by nanomaterial-based electrochemical (bio)sensors.<sup>199</sup> For the development of electrochemical, chemiresistive, and wearable sensors, tin oxide nanomaterials have been increasingly applied as an electrode modifier due to their unique properties including abundant ability, biocompatibility, cost-effective, excellent bandgap, and thermal stability.<sup>200</sup> Additionally, wireless technology is also important to design a seamless digital interface for the communication between biomedical sensors and external receivers. For example, the emerging wireless chemical sensors, combining sensing and wireless data transfer systems (e.g., a wireless potentiostat), facilitate mobile *cavitas* sensing applications. The wireless potentiostat is remarkably contributing to advancements in modern-style diagnosis in healthcare and sports sectors and mobile PoC diagnostics. Importantly, the wireless device links to a unique feature for evolving smart health Internet of Things (IoT).<sup>195,196</sup> The key considerations to achieving such advanced electronics coupled with digital systems are size, weight, power consumption, battery lifetime, and connectivity, rather than focusing on solely the analytical performance of the traditional devices.

Challengingly, the miniaturization of wearable sensing devices to fit firmly inside the mouth for *cavitas* applications also limits the footprint to accommodate the powering system. Scaling down the traditional power source (e.g., batteries) to match the *cavitas* device or small electronics is difficult. It is, thus, urgent to explore novel and reliable solutions for such sufficient powering systems to increase their lifespan and energy performances while decreasing the volume of the device.<sup>203</sup> Energy technology is another key to supporting the successful development of smart sensors.

The emerging concept of energy harvesting enables the development of self-powered devices that harvest energy from the environment for powering the device itself and/or charging batteries/supercapacitors. Many research groups have demonstrated various energy harvesting methods for self-power devices.<sup>204</sup> For example, biofuel cells (BFCs) can convert biochemical energy from various “renewable” biochemical species into sustainable electrical energy with the assistance of biological components (e.g., enzymes), thus offering an emerging “green” alternative for applications. The utilization of BFCs as integrated power sources holds a great promise for biomedical device applications.<sup>205,206</sup> Additionally, piezoelectric materials can also be used as mechanisms that generate

electrical energy through mechanical deformation. The existing example of harvesting from motions of internal organs (i.e., heart, lung, and diaphragm) achieved a power density of  $0.18 \mu\text{W cm}^{-2}$  in the heart.<sup>207</sup> In addition to piezoelectric materials, mechanical energy can be transformed into electricity by triboelectric energy harvesters via triboelectric effect and electrostatic induction.<sup>208</sup> A thermoelectric-based energy harvester is an alternative for energy harvesting that converts thermal energy into electric power through a temperature gradient. Moreover, the emerging wireless power transfer system is an alternative technology to satisfy the power needs of miniaturized bioelectronic devices that can deliver the energy from external dedicated power sources to the target device (at a sensing system unit) over a distance without traditional interconnecting wires.<sup>209</sup>

In addition to hardware units, computer algorithms and processing units are also important.<sup>210</sup> The essential property of any sensor is to detect and provide accurate information about the target analyte. Current research attempts have been made to realize an array of sensors including multisignal readout. The increased number of sensors or signals results in high data throughputs, representing a challenge to effectively process such a huge amount of sensory information.<sup>211</sup> Hence, we need machine learning—a recent technology in artificial intelligence (AI). Machine learning involves computer algorithms that can improve themselves automatically through experience and training data (i.e., a built model from sample data by the machine learning algorithms). The algorithms can learn and automate the extraction of patterns, and functions according to a given dataset which usually requires a domain expert to assess. In the case of mouthguard sensors, the feedback helps wearers know their health status from the reported analyte concentration and/or plan for treatments. This idea becomes a promising alternative that replaces traditional sensing strategies with enlarging datasets and confusing system models. For example, the use of machine learning algorithms is expected to allow mouthguard sensors and point-of-need salivary sensors to diagnose several types of diseases in a noninvasive, convenient, and inexpensive way when compared with those traditional methods.<sup>208</sup> Additionally, the significant processed results can be linked via smart networks to clinical sectors, trainers, and the family to make timely decisions and improve the health quality.

A proof-of-concept demonstration of a smart “Sense-Act-Treat” system is closed-loop insulin delivery as the artificial pancreas.<sup>209</sup> This emerging system has pioneered and further enabled many practical systems to meet relevant “Sense-Act-Treat” situations. The



idea of integrating a *cavitas* sensor, a control algorithm, and a treating device (e.g., a drug delivery pump) together could facilitate real-time continuous feedback and treatment. The obtained physical and biochemical information at the sensor can be transferred to a control algorithm and sent to the wearer. The rapid-acting analogs for subcutaneous treatment at a treating device are according to real-time target analyte levels and modulated by a control algorithm. The use of wireless technologies for communication between the integrated components will allow an automated data exchange between components without the need for human intervention. Most current available devices can only continuously monitor a limited number of targets such as physical signals (e.g., pressure and temperature) and common analytes (e.g., glucose and uric acid). However, saliva involves many other detectable target analytes (e.g., proteins, enzymes, lipids, and pathogens). In this regard, the development of *cavitas* sensors that can continuously monitor a broad spectrum of target analytes with on-device processing is desirable and will provide tremendous benefits to the healthcare system. We should consider many challenging factors for translating lab-in-a-mouth sensors and point-of-need sensors from research laboratories to clinical applications and real markets, such as user-friendly interface, complex environment in real scenarios,<sup>212</sup> as well as analytical chemistry aspects (e.g., sample preparation and matrix effects).

Along with technological advances in various fields mentioned above, we expect future research to focus on expanding the target biomarker and analyzing various biomarkers at once to increase their performance and applicability. In addition, for those wearable sensors meant to be implanted or worn for real-time continuous monitoring of users' health status, we should explore safe and biocompatible materials and recognition elements that can prevent biofouling. Finally, yet importantly, various obstacles that can occur in daily life, such as food intake, intraoral bleeding, changes in saliva secretion, and changes in saliva concentration, should also be considered in developing sensors. These things will eventually change the future of salivary wearable technology as it can evolve the monitoring process.

### Acknowledgments

We acknowledge the support from National Research Council of Thailand (NRCT (grant number: N41A640129), Prince of Songkla University, Hat Yai, Thailand, and Align Technology, Inc. We would like to thank the Talent Management Project of Prince of Songkla University, and the Center of Excellence for Innovation in Chemistry (PERCH-CIC), Ministry of Higher Education, Science, Research, and Innovation (MHESI).

### ORCID

Dinesh Rokaya  <https://orcid.org/0000-0002-3854-667X>  
 Itthipon Jeerapan  <https://orcid.org/0000-0001-8016-6411>

### References

1. Y.-H. Lee and D. T. Wong, *American Journal of Dentistry*, **22**, 241 (2009), <https://ncbi.nlm.nih.gov/pmc/articles/PMC2860957/>.
2. N. Spielmann and D. T. Wong, *Oral Diseases*, **17**, 345 (2011).
3. S. P. Humphrey and R. T. Williamson, *The Journal of Prosthetic Dentistry*, **85**, 162 (2001).
4. J. Liu and Y. Duan, *Oral Oncology*, **48**, 569 (2012).
5. S. Sujatha, U. Jalihal, Y. Devi, N. Rakesh, P. Chauhan, and S. Sharma, *Indian Journal of Gastroenterology*, **35**, 186 (2016).
6. K. Ngamchuea, K. Chaisiwamongkhon, C. Batchelor-McAuley, and R. G. Compton, *Analyst*, **143**, 81 (2018).
7. A. Ilea, V. Andrei, C. N. Feurdean, A.-M. Băbțan, N. B. Petrescu, R. S. Cămpian, A. B. Bosca, B. Ciui, M. Tertis, and R. Săndulescu, *Biosensors*, **9**, 27 (2019).
8. S. Prasad, A. K. Tyagi, and B. B. Aggarwal, *Experimental Biology and Medicine*, **241**, 783 (2016).
9. N. Rathnayake, D.-R. Gieselmann, A. M. Heikkinen, T. Tervahartiala, and T. Sorsa, *Diagnostics*, **7**, 7 (2017).
10. M. Choromańska, A. Klimiuk, P. Kostecka-Sochoń, K. Wilczyńska, M. Kwiatkowski, N. Okuniewska, N. Waszkiewicz, A. Zalewska, and M. Maciejczyk, *Int. J. Mol. Sci.*, **18** (2017).
11. P. Buczko, A. Zalewska, and I. Szarmach, *J Physiol Pharmacol*, **66**, 3 (2015), <https://europepmc.org/article/med/25716960>.
12. K. Avezov, A. Z. Reznick, and D. Aizenbud, *Respir. Physiol. Neurobiol.*, **209**, 91 (2015).
13. H. Graf, *Helv. odont. Acta*, **10**, 94 (1966).
14. H. Graf and H. R. Mühlemann, *Archives of Oral Biology*, **14**, 259 (1969).
15. V. Shetty, C. Zigler, T. F. Robles, D. Elashoff, and M. Yamaguchi, *Psychoneuroendocrinology*, **36**, 193 (2011).
16. M. S. Mannoor, H. Tao, J. D. Clayton, A. Sengupta, D. L. Kaplan, R. R. Naik, N. Verma, F. G. Omenetto, and M. C. McAlpine, *Nat. Commun.*, **3**, 763 (2012).
17. J. Kim, G. Valdés-Ramírez, A. J. Bandodkar, W. Jia, A. G. Martinez, J. Ramírez, P. Mercier, and J. Wang, *Analyst*, **139**, 1632 (2014).
18. A. Roda, E. Michelini, L. Cevenini, D. Calabria, M. M. Calabretta, and P. Simoni, *Anal. Chem.*, **86**, 7299 (2014).
19. J. Kim, S. Imani, W. R. de Araujo, J. Warchall, G. Valdés-Ramírez, T. R. L. C. Paixão, P. P. Mercier, and J. Wang, *Biosens. Bioelectron.*, **74**, 1061 (2015).
20. M. Zangheri, L. Cevenini, L. Anfossi, C. Baggiani, P. Simoni, F. Di Nardo, and A. Roda, *Biosens. Bioelectron.*, **64**, 63 (2015).
21. T. Arakawa et al., *Biosens. Bioelectron.*, **84**, 106 (2016).
22. Y. Jia, H. Sun, X. Li, D. Sun, T. Hu, N. Xiang, and Z. Ni, *Biomed. Microdevices*, **20**, 89 (2018).
23. Y. Lee et al., *Proc. Natl Acad. Sci.*, **115**, 5377 (2018).
24. L. F. de Castro, S. V. de Freitas, L. C. Duarte, J. A. C. de Souza, T. R. Paixão, and W. K. Coltro, *Anal. Bioanal. Chem.*, **411**, 4919 (2019).
25. B. Ciui, M. Tertis, C. N. Feurdean, A. Ilea, R. Sandulescu, J. Wang, and C. Cristea, *Sensors Actuators B*, **281**, 399 (2019).
26. T. Arakawa, K. Tomoto, H. Niita, K. Toma, S. Takeuchi, T. Sekita, S. Minakuchi, and K. Mitsubayashi, *Anal. Chem.*, **92**, 12201 (2020).
27. R. Kinjo, T. Wada, H. Churei, T. Ohmi, K. Hayashi, K. Yagishita, M. Uo, and T. Ueno, *Sensors*, **21**, 1503 (2021).
28. R. Sangsawang, C. Buranachai, P. Thavarungkul, P. Kanatharana, and I. Jeerapan, *Microchim. Acta*, **188**, 1 (2021).
29. R. M. Torrente-Rodríguez, H. Lukas, J. Tu, J. Min, Y. Yang, C. Xu, H. B. Rossiter, and W. Gao, *Matter*, **3**, 1981 (2020).
30. B. Ning, T. Yu, S. Zhang, Z. Huang, D. Tian, Z. Lin, A. Niu, N. Golden, K. Hensley, and B. Threton, *Sci. Adv.*, **7**, eabe3703 (2021).
31. M. D. Torres, W. R. de Araujo, L. F. de Lima, A. L. Ferreira, and C. de la Fuente-Nunez, *Matter*, **4**, 2403 (2021).
32. N. K. Singh, P. Ray, A. F. Carlin, C. Magallanes, S. C. Morgan, L. C. Laurent, E. S. Aronoff-Spencer, and D. A. Hall, *Biosens. Bioelectron.*, **180**, 113111 (2021).
33. J. P. Hunt, E. L. Zhao, T. J. Free, M. Soltani, C. A. Warr, A. B. Benedict, M. K. Takahashi, J. S. Griffiths, W. G. Pitt, and B. C. Bundy, *New Biotechnol.*, **66**, 53 (2022).
34. D. M. Heithoff, L. Barnes, S. P. Mahan, G. N. Fox, K. E. Arn, S. J. Ettinger, A. M. Bishop, L. N. Fitzgibbons, J. C. Fried, and D. A. Low, *JAMA network open*, **5**, e2145669 (2022).
35. M. S. Mannoor, H. Tao, J. D. Clayton, A. Sengupta, D. L. Kaplan, R. R. Naik, N. Verma, F. G. Omenetto, and M. C. McAlpine, *Nat. Commun.*, **3**, 1 (2012).
36. D. Ma, C. Mason, and S. S. Ghoreishizadeh, *2017 IEEE Biomedical Circuits and Systems Conference (BioCAS)*, "p. 1–4, 201719–21 (2017).
37. S. Maheshwaran, M. Akilarasan, S.-M. Chen, T.-W. Chen, E. Tamilalagan, C. Y. Tzu, and B.-S. Lou, *J. Electrochem. Soc.*, **167**, 066517 (2020).
38. P. Limsakul, K. Charupanit, C. Moonla, and I. Jeerapan, *Emergent Materials*, **4**, 231 (2021).
39. Z. Khurshid, M. Naseem, Z. Sheikh, S. Najeeb, S. Shahab, and M. S. Zafar, *Saudi Pharmaceutical Journal: SPJ: the Official Publication of the Saudi Pharmaceutical Society*, **24**, 515 (2016).
40. C. Hollins, *Basic Guide to Anatomy and Physiology for Dental Care Professionals* (Wiley, New York) (2012).
41. E. N. Marieb, *Essential of Human Anatomy and Physiology* (Benjamin Cummings, San Francisco: USA) (2003).
42. A. Nanci and T. Cate's, *Oral Histology: Development, Structure, and Function* (Mosby, St Louis, USA) (2003).
43. C. L. B. Lavelle, *Applied Oral Physiology*, ed. C. L. B. Lavelle (Butterworth-Heinemann) 2nd ed., p. 12 (1988).
44. J. P. Okeson, *Management of Temporomandibular Disorders and Occlusion* (Elsevier, Amsterdam) (2013).
45. E. Solaberrieta, A. Garmendia, A. Brizuela, J. R. Otegi, G. Pradies, and A. Szentpétery, *BioMed Res. Int.*, **2016**, 7173824 (2016).
46. E. Bando, K. Nishigawa, M. Nakano, H. Takeuchi, S. Shigemoto, K. Okura, T. Satsuma, and T. Yamamoto, *Jpn Dent Sci Rev*, **45**, 83 (2009).
47. K. I. Afrashtehfar and S. Qadeer, *Cranio: the Journal of Craniomandibular Practice*, **34**, 52 (2016).
48. R. B. Kerstein, *Cranio: the Journal of Craniomandibular Practice*, **22**, 96 (2004).
49. E. Solaberrieta, J. R. Otegi, N. Goicoechea, A. Brizuela, and G. Pradies, *J Prosthet Dent*, **114**, 92 (2015).
50. L. C. Schenkels, E. C. Veerman, and A. V. Nieuw Amerongen, *American Association of Oral Biologists*, **6**, 161 (1995).
51. W. M. Edgar, *British Dental Journal*, **172**, 305 (1992).
52. V. de Almeida Pdel, A. M. Grégio, M. A. Machado, A. A. de Lima, and L. R. Azevedo, *The Journal of Contemporary Dental Practice*, **9**, 72 (2008).
53. G. H. Carpenter, *Annual Review of Food Science and Technology*, **4**, 267 (2013).
54. T. Pfaffe, J. Cooper-White, P. Beyerlein, K. Kostner, and C. Punyadeera, *Clin. Chem.*, **57**, 675 (2011).
55. A. Aguirre, L. A. Testa-Weintraub, J. A. Banderas, G. G. Haraszthy, M. S. Reddy, and M. J. Levine, *Critical Reviews in Oral Biology & Medicine*, **4**, 343 (1993).



56. I. D. Mandel, *Journal of Oral Pathology & Medicine*, **19**, 119 (1990).
57. J. L. Chicharro, A. Lucía, M. Pérez, A. F. Vaquero, and R. Ureña, *Sports Medicine*, **26**, 17 (1998).
58. E. Kaufman and I. B. Lamster, *Critical Reviews in Oral Biology & Medicine*, **13**, 197 (2002).
59. C. F. Streckfus and L. R. Bigler, *Oral Diseases*, **8**, 69 (2002).
60. S. Chiappin, G. Antonelli, R. Gatti, and E. F. De Palo, *Clin. Chim. Acta*, **383**, 30 (2007).
61. R. S. P. Malon, S. Sadir, M. Balakrishnan, and E. P. Córcoles, *BioMed Res. Int.*, **2014**, 962903 (2014).
62. I. Jeeran, T. Sonsa-ard, and D. Nacapricha, *Chemosensors*, **8**, 71 (2020).
63. R. Gatti and E. F. De Palo, *Scandinavian Journal of Medicine & Science in Sports*, **21**, 157 (2011).
64. S. Meenu, S. Sayanti, B. Mayank, Y. Pragzna, and B. Dharmadev, *Int J Pharm Biol Arch*, **5**, 1 (2014).
65. B. Viswanath, C. S. Choi, K. Lee, and S. Kim, *TrAC, Trends Anal. Chem.*, **89**, 60 (2017).
66. K. Shibasaki, M. Kimura, R. Ikarashi, A. Yamaguchi, and T. Watanabe, *Metabolomics*, **8**, 484 (2012).
67. M. Soukup, I. Biesiada, A. Henderson, B. Idowu, D. Rodeback, L. Ridpath, E. G. Bridges, A. M. Nazar, and K. G. Bridges, *Diabetology & Metabolic Syndrome*, **4**, 14 (2012).
68. W. L. Nyhan, *Journal of Inherited Metabolic Disease*, **20**, 171 (1997).
69. M. E. Moran, *Front Biosci*, **8**, s1339 (2003).
70. G. F. Falasca, *Clinics in Dermatology*, **24**, 498 (2006).
71. T. Nakagawa et al., *Am. J. Physiol. Renal Physiol.*, **290**, F625 (2006).
72. T. R. Merriman and N. Dalbeth, *Joint Bone Spine*, **78**, 35 (2011).
73. R. Segura, C. Javierre, J. L. Ventura, M. A. Lizarraga, B. Campos, and E. Garrido, *Br. J. Sports Med.*, **30**, 305 (1996).
74. R. V. T. Santos, A. L. R. Almeida, E. C. Caperuto, E. Martins, and L. F. B. P. Costa Rosa, *Comp. Biochem. Physiol. B: Biochem. Mol. Biol.*, **145**, 114 (2006).
75. A. Soni and S. K. Jha, *Biosens. Bioelectron.*, **67**, 763 (2015).
76. T. Arakawa, Y. Kuroki, H. Nitta, P. Chouhan, K. Toma, S.-I. Sawada, S. Takeuchi, T. Sekita, K. Akiyoshi, and S. Minakuchi, *Biosens. Bioelectron.*, **84**, 106 (2016).
77. L. García-Carmona, A. Martín, J. R. Sempionatto, J. R. Moreto, M. C. González, J. Wang, and A. Escarpa, *Anal. Chem.*, **91**, 13883 (2019).
78. Ç. Çiçek, F. Yılmaz, E. Özgür, H. Yavuz, and A. Denizli, *Chemosensors*, **4**, 21 (2016).
79. W. Xiao, D. Zhi, Q. Pan, Y. Liang, F. Zhou, and Z. Chen, *Anal. Methods*, **12**, 5691 (2020).
80. C. Song, Y. Li, B. Wang, Y. Hong, C. Xue, Q. Li, E. Shen, and D. Cui, *Colloids Surf., B*, **197**, 111430 (2021).
81. M.-H. Mirzaii Dizgah, M.-R. Mirzaii Dizgah, I. Mirzaii-Dizgah, H. Lachinani, B. Dormanesh, and M. Veisizadeh, *Avicenna J Dent Res*, **11**, 79 (2019).
82. F. Parnianchi, S. Kashanian, M. Nazari, C. Santoro, P. Bollella, and K. Varmira, *Microchem. J.*, **168**, 106367 (2021).
83. S. Karjalainen, L. Sewón, E. Soderling, B. Larsson, I. Johansson, O. Simell, H. Lapinleimu, and R. Seppänen, *J. Dent. Res.*, **76**, 1637 (1997).
84. S. Singh, V. Ramesh, N. Oza, P. D. Balamurali, K. V. Prashad, and P. Balakrishnan, *J Oral Maxillofac Pathol*, **18**, 4 (2014).
85. Y. J. Lee, K. S. Eom, K.-S. Shin, J. Y. Kang, and S. H. Lee, *Sensors Actuators B*, **271**, 73 (2018).
86. B. Štabuc, L. Vrhovc, M. Štabuc-Šilih, and T. E. Cizej, *Clin. Chem.*, **46**, 193 (2000).
87. M. Barton and A. Sorokin, *Seminars in Nephrology*, **35**, 156 (2015).
88. D. O. Temilola, K. Bezuidenhout, R. T. Erasmus, L. Stephen, M. R. Davids, and H. Holmes, *BMC Nephrology*, **20**, 387 (2019).
89. S. Kalasin, P. Sangnuang, P. Khownarumit, I. M. Tang, and W. Surareungchai, *ACS Biomaterials Science & Engineering*, **6**, 5895 (2020).
90. C. Labat, S. Thul, J. Pirault, M. Temmar, S. N. Thornton, A. Benetos, and M. Bäck, *Disease Markers*, **2018**, 3152146 (2018).
91. P. D. Beer and P. A. Gale, *Angew. Chem. Int. Ed.*, **40**, 486 (2001).
92. A. Oliveby, F. Lagerlöf, J. Ekstrand, and C. Dawes, *Caries Research*, **23**, 243 (1989).
93. F. S. Apple et al., *Circulation*, **116**, e95 (2007).
94. D. Kwon, T.-I. Lee, J. Shim, S. Ryu, M. S. Kim, S. Kim, T.-S. Kim, and I. Park, *ACS Appl. Mater. Interfaces*, **8**, 16922 (2016).
95. D. A. Granger, K. T. Kivlighan, M. El-Sheikh, E. B. Gordis, and L. R. Stroud, *Ann. N.Y. Acad. Sci.*, **1098**, 122 (2007).
96. A. van Stegeren, N. Rohleder, W. Everaerd, and O. T. Wolf, *Psychoneuroendocrinology*, **31**, 137 (2006).
97. U. M. Nater, R. La Marca, L. Florin, A. Moses, W. Langhans, M. M. Koller, and U. Ehler, *Psychoneuroendocrinology*, **31**, 49 (2006).
98. N. Takai, M. Yamaguchi, T. Aragaki, K. Eto, K. Uchihashi, and Y. Nishikawa, *Ann. N.Y. Acad. Sci.*, **1098**, 510 (2007).
99. M. Yamaguchi and J. Sakakima, *Journal of International Medical Research*, **35**, 91 (2007).
100. J. M. Wolf, E. Nicholls, and E. Chen, *Biological Psychology*, **78**, 20 (2008).
101. N. Rohleder, J. M. Wolf, E. F. Maldonado, and C. Kirschbaum, *Psychophysiology*, **43**, 645 (2006).
102. J. A. DeCaro, *American Journal of Human Biology*, **20**, 617 (2008).
103. H.-Y. Hsiao, R. L. C. Chen, C.-C. Chou, and T.-J. Cheng, *Sensors*, **19**, 1571 (2019).
104. V. P. Rodrigues, M. M. Franco, C. P. Marques, R. C. de Carvalho, S. A. Leite, A. L. Pereira, and B. B. Benatti, *Archives of oral biology*, **62**, 58 (2016).
105. M. R. Koduru, A. Ramesh, S. Adapa, and J. Shetty, *Annals of Medical and Health Sciences Research*, **7**, 337 (2017), <https://amhsr.org/articles/salivary-albumin-as-a-biomarker-for-oral-squamous-cell-carcinoma-and-chronic-periodontitis-3708.html>.
106. H. M. E. Azzazy and R. H. Christenson, *Clin. Chem.*, **43**, 2014a (1997).
107. P. B. Vaziri, M. Vahedi, S. Abdollahzadeh, H. Abdolsamadi, M. Hajilooi, and S. Kasraee, *Iranian journal of public health*, **38**, 54 (2009), <https://ijph.tums.ac.ir/index.php/ijph/article/view/3171>.
108. R. Metgud and S. Patel, *Biotechnic & Histochemistry*, **89**, 8 (2014).
109. D. Soo-Quee Koh and G. Choon-Huat Koh, *Occupational and Environmental Medicine*, **64**, 202 (2007).
110. M. Rizwan, D. Koh, M. A. Booth, and M. U. Ahmed, *Sensors Actuators B*, **255**, 557 (2018).
111. G. Virella, J. Goudswaard, and R. Boackle, *Clin. Chem.*, **24**, 1421 (1978).
112. S. Perera, M. Uddin, and J. A. Hayes, *International Journal of Behavioral Medicine*, **4**, 170 (1997).
113. T. Di Giulio, E. Mazzotta, and C. Malitesta, *Biosensors*, **11**, 3 (2021).
114. M. Sekar, R. Sriramprabha, P. K. Sekhar, S. Bhansali, N. Ponpandian, M. Pandiaraj, and C. Viswanathan, *J. Electrochem. Soc.*, **167**, 067508 (2020).
115. E.-M. Poll, I. Kreitschmann-Andermahr, Y. Langejuergen, S. Stanzel, J. M. Gilsbach, A. Gressner, and E. Yagmur, *Clin. Chim. Acta*, **382**, 15 (2007).
116. S. Dalirirad, D. Han, and A. J. Steckl, *ACS omega*, **5**, 32890 (2020).
117. K. Inoue, P. Ferrante, Y. Hirano, T. Yasukawa, H. Shiku, and T. Matsue, *Talanta*, **73**, 886 (2007).
118. E. R. Cooper, K. C. Y. McGrath, and A. K. Heather, *Sensors*, **13**, 2148 (2013).
119. J. Vittek, D. G. L'Hommedieu, G. G. Gordon, S. C. Rappaport, and A. L. Southren, *Life Sci.*, **37**, 711 (1985).
120. O. Laczka, F. J. del Campo, F. X. Muñoz-Pascual, and E. Baldrich, *Anal. Chem.*, **83**, 4037 (2011).
121. P. M. Meulenber and J. A. Hofman, *Clin. Chem.*, **35**, 168 (1989).
122. J. G. Lewis, *Clin Biochem Rev*, **27**, 139 (2006), <https://ncbi.nlm.nih.gov/pmc/articles/PMC1579286/>.
123. J. Robbins and J. E. Rall, *Recent Progress in Hormone Research*, **13**, 161 (1957), <https://pubmed.ncbi.nlm.nih.gov/13477808/>.
124. R. Ekins, *Lancet*, **325**, 1129 (1985).
125. C. M. Mendel, *Endocrine Reviews*, **10**, 232 (1989).
126. J. K. M. Aps and L. C. Martens, *Forensic Sci. Int.*, **150**, 119 (2005).
127. R. P. Shellis, *Archives of Oral Biology*, **23**, 485 (1978).
128. V. W. H. Leung and B. W. Darvell, *Journal of Dentistry*, **25**, 475 (1997).
129. J.-M. Meyer, *Corros. Sci.*, **17**, 971 (1977).
130. K. Elaghi, M. Traisnel, and H. F. Hildebrand, *Electrochim. Acta*, **38**, 1769 (1993).
131. B. Levallois, Y. Fovet, L. Lapeyre, and J. Y. Gal, *Dent. Mater.*, **14**, 441 (1998).
132. J.-Y. Gal, Y. Fovet, and M. Adib-Yadzi, *Talanta*, **53**, 1103 (2001).
133. F. C. Giacomelli, C. Giacomelli, and A. Spinelli, *J. Braz. Chem. Soc.*, **15**, 541 (2004).
134. J. Klimek, E. Hellwig, and G. Ahrens, *Caries Research*, **16**, 156 (1982).
135. H. Nordbø, S. Darwish, and R. S. Bhatnagar, *European Journal of Oral Sciences*, **92**, 306 (1984).
136. H. Uchida and C. E. Ovit, *The Journal of Prosthetic Dentistry*, **127**, 383 (2021).
137. R. M. Nagler, O. Hershkovich, S. Lischinsky, E. Diamond, and A. Z. Reznick, *Journal of Investigative Medicine*, **50**, 214 (2002).
138. K. Ngamchuea, C. Batchelor-McAuley, and R. G. Compton, *Sensors Actuators B*, **262**, 404 (2018).
139. T. J. Lasisi, *African Journal of Medicine and Medical Sciences*, **43**, 347 (2014), <https://pubmed.ncbi.nlm.nih.gov/26234123/>.
140. K. S. Eom, Y. J. Lee, H. W. Seo, J. Y. Kang, J. S. Shim, and S. H. Lee, *Analyst*, **145**, 908 (2020).
141. D. Pandya, A. K. Nagrajappa, and K. S. Ravi, *J Clin Diagn Res*, **10**, ZC58 (2016).
142. É. Tékus, M. Kaj, E. Szabó, N. Szénási, I. Kerepesi, M. Figler, R. Gábrriel, and M. Wilhelm, *Acta Biologica Hungarica*, **63**, 89 (2012).
143. S. Tsujita and K. Morimoto, *Environmental Health and Preventive Medicine*, **4**, 1 (1999).
144. E. S. Frenkel and K. Ribbeck, *Journal of Oral Microbiology*, **7**, 29759 (2015).
145. F. Agha-Hosseini, M. Imanpour, I. Mirzaii-Dizgah, and M.-S. Moosavi, *Sci. Rep.*, **7**, 12060 (2017).
146. M. L. Byrne, N. M. O'Brien-Simpson, E. C. Reynolds, K. A. Walsh, K. Laughton, J. M. Waloszek, M. J. Woods, J. Trinder, and N. B. Allen, *Brain, Behavior, and Immunity*, **34**, 164 (2013).
147. M. Wang, Z. Chen, X. Jing, H. Zhou, Y. Wang, J. Ye, and Q. Chu, *J. Chromatogr. B*, **1176**, 122756 (2021).
148. S. Clifton et al., *The Journal of Clinical Endocrinology & Metabolism*, **101**, 3939 (2016).
149. B. K. Gandara, L. Leresche, and L. Mancl, *Ann. N.Y. Acad. Sci.*, **1098**, 446 (2007).
150. D. Vozgirdaite, H. Ben Halima, F. G. Bellagambi, A. Alcacer, F. Palacio, N. Jaffrezic-Renault, N. Zine, J. Bausells, A. Elaissari, and A. Errachid, *Chemosensors*, **9**, 26 (2021).
151. L. Barhoumi, A. Baraket, F. G. Bellagambi, G. S. Karanasiou, M. B. Ali, D. I. Fotiadis, J. Bausells, N. Zine, M. Sigaud, and A. Errachid, *Sensors Actuators B*, **266**, 477 (2018).
152. L. Barhoumi, F. G. Bellagambi, F. M. Vivaldi, A. Baraket, Y. Clément, N. Zine, M. Ben Ali, A. Elaissari, and A. Errachid, *Sensors*, **19**, 692 (2019).
153. F. G. Bellagambi, A. Baraket, A. Longo, M. Vatteroni, N. Zine, J. Bausells, R. Fuoco, F. Di Francesco, P. Salvo, and G. S. Karanasiou, *Sensors Actuators B*, **251**, 1026 (2017).
154. L. L. Fernandes et al., *J. Dent. Res.*, **99**, 1435 (2020).

155. K. F. Hung, Y. C. Sun, B. H. Chen, J. F. Lo, C. M. Cheng, C. Y. Chen, C. H. Wu, and S. Y. Kao, *Journal of the Chinese Medical Association: JCMA*, **83**, 891 (2020).
156. L. F. Gabler, S. H. Huddleston, N. Z. Dau, D. J. Lessley, K. B. Arbogast, X. Thompson, J. E. Resch, and J. R. Crandall, *Ann. Biomed. Eng.*, **48**, 2599 (2020).
157. A. G. Domel et al., *Sci. Rep.*, **11**, 7501 (2021).
158. L. F. Gabler, N. Z. Dau, G. Park, A. Miles, K. B. Arbogast, and J. R. Crandall, *Ann. Biomed. Eng.*, **49**, 2760 (2021).
159. J. J. Kim, G. R. Stafford, C. Beauchamp, and S. A. Kim, *Sensors*, **20**, 3953 (2020).
160. P. F. Nascimento, A. P. Franco, R. Fiorin, M. A. D. Souza, H. J. Kalinowski, and I. Abe, *Journal of Microwaves, Optoelectronics and Electromagnetic Applications*, **17**, 306 (2018).
161. R. Goldoni, A. Scolaro, E. Boccalari, C. Dolci, A. Scarano, F. Inchingolo, P. Ravazzani, P. Muti, and G. Tartaglia, *Biosensors*, **11**, 396 (2021).
162. H.-R. Lim, S. M. Lee, S. Park, C. Choi, H. Kim, J. Kim, M. Mahmood, Y. Lee, J.-H. Kim, and W.-H. Yeo, *Biosens. Bioelectron.*, **210**, 114329 (2022).
163. A. Roda, S. Cavallera, F. Di Nardo, D. Calabria, S. Rosati, P. Simoni, B. Colitti, C. Baggiani, M. Roda, and L. Anfossi, *Biosens. Bioelectron.*, **172**, 112765 (2021).
164. S. Gupta, M. T. Nayak, J. D. Sunitha, G. Dawar, N. Sinha, and N. S. Rallan, *J Oral Maxillofac Pathol*, **21**, 334 (2017).
165. B. N. V. S. Satish, P. Srikala, B. Maharudrappa, S. M. Awanti, P. Kumar, and D. Hugar, *J Int Oral Health*, **6**, 114 (2014), <https://ncbi.nlm.nih.gov/pmc/articles/PMC4037799/>.
166. L. Temmerman, A. M. De Livera, J. B. Bowne, J. R. Sheedy, D. L. Callahan, A. Nahid, D. P. De Souza, L. Schoofs, D. L. Tull, and M. J. McConville, *Journal of Diabetes & Metabolism*, **4**, 2 (2012).
167. W. Zhang, Y. Du, and M. L. Wang, *Sensing and Bio-Sensing Research*, **4**, 23 (2015).
168. J. Noiphung, M. P. Nguyen, C. Punyadeera, Y. Wan, W. Laiwattanapaisal, and C. S. Henry, *Theranostics*, **8**, 3797 (2018).
169. M. Yamaguchi, M. Mitsumori, and Y. Kano, *IEEE Eng. Med. Biol. Mag.*, **17**, 59 (1998).
170. R. Agrawal, N. Sharma, M. Rathore, V. Gupta, S. Jain, V. Agarwal, and S. Goyal, *J Diabetes Metab*, **4**, 266 (2013).
171. C. Jurysta, N. Bulur, B. Oguzhan, I. Satman, T. M. Yilmaz, W. J. Malaisse, and A. Sener, *J. Biomed. Biotechnol.*, **2009**, 430426 (2009).
172. M. J. A. Campbell, *Archives of Oral Biology*, **10**, 197 (1965).
173. P. Abikshyeet, V. Ramesh, and N. Oza, *Diabetes Metab Syndr Obes*, **5**, 149 (2012).
174. J. Yeom, A. Choe, S. Lim, Y. Lee, S. Na, and H. Ko, *Sci. Adv.*, **6**, eaba5785 (2020).
175. E. V. Adlin, A. D. Marks, and B. J. Channick, *Clinical and Experimental Hypertension. Part A: Theory and Practice*, **4**, 1869 (1982).
176. D. P. Lauer, R. B. Hickler, and G. W. Thorn, *New Engl. J. Med.*, **267**, 1136 (1962).
177. K. J. Manley, *Journal of Renal Care*, **40**, 172 (2014).
178. P. Faragó, R. Gálátus, S. Hintea, A. B. Boşca, C. N. Feurdean, and A. Ilea, *Sensors*, **19**, 4719 (2019).
179. R. K. Mishra et al., *Talanta*, **211**, 120757 (2020).
180. K. Saisahas et al., *Nanomaterials*, **12**, 73 (2022).
181. A. N. Ramdzan, M. I. G. S. Almeida, M. J. McCullough, and S. D. Kolev, *Anal. Chim. Acta*, **919**, 47 (2016).
182. P. Tseng, B. Napier, L. Garbarini, D. L. Kaplan, and F. G. Omenetto, *Adv. Mater.*, **30**, 1703257 (2018).
183. T. Ji et al., *Biosens. Bioelectron.*, **166**, 112455 (2020).
184. F. Pena-Pereira, I. Lavilla, and C. Bendicho, *Talanta*, **147**, 390 (2016).
185. T. Ozer, B. J. Geiss, and C. S. Henry, *J. Electrochem. Soc.*, **167**, 037523 (2019).
186. N. Malathi, S. Mythili, and H. R. Vasanthi, *International Scholarly Research Notices*, **2014**, 1 (2014).
187. J. Mairhofer, K. Roppert, and P. Ertl, *Sensors*, **9**, 4804 (2009).
188. P. Belgrader, W. Bennett, D. Hadley, J. Richards, P. Stratton, R. Mariella Jr, and F. Milanovich, *Science*, **284**, 449 (1999).
189. I. Jeerapan, C. Moonla, P. Thavarungkul, and P. Kanatharana, *Prog. Mol. Biol. Transl. Sci.*, ed. A. Pandya and V. Singh (Academic Press, New York) Vol. 187, p. 249 (2022).
190. G. Xun, S. T. Lane, V. A. Petrov, B. E. Pepa, and H. Zhao, *Nat. Commun.*, **12**, 1 (2021).
191. J. T. Wu, K. Leung, and G. M. Leung, *Lancet*, **395**, 689 (2020).
192. H. Tombuloglu, H. Sabit, E. Al-Suhaimi, R. Al Jindan, and K. R. Alkharsah, *PLoS One*, **16**, e0250942 (2021).
193. L. Azzi, V. Maurino, A. Baj, M. Dani, A. d'Aiuto, M. Fasano, M. Lualdi, F. Sessa, and T. Alberio, *J. Dent. Res.*, **100**, 115 (2021).
194. A. P. F. Turner, *ECS Sensors Plus*, **1**, 011601 (2022).
195. A. Scott, R. Pandey, S. Saxena, E. Osman, Y. Li, and L. Soleymani, *ECS Sensors Plus*, **1**, 014601 (2022).
196. V. Chaudhary, A. Kaushik, H. Furukawa, and A. Khosla, *ECS Sensors Plus*, **1**, 013601 (2022).
197. I. Jeerapan and S. Poorahong, *J. Electrochem. Soc.*, **167**, 037573 (2020).
198. F. Da Silva Santos, L. Vitor da Silva, P. V. S. Campos, C. de Medeiros Strunkis, C. M. G. Ribeiro, and M. O. Salles, *ECS Sensors Plus*, **1**, 013603 (2022).
199. L. Qian, S. Durairaj, S. Prins, and A. Chen, *Biosens. Bioelectron.*, **175**, 112836 (2021).
200. A. Sharma, A. Ahmed, A. Singh, S. K. Oruganti, A. Khosla, and S. Arya, *J. Electrochem. Soc.*, **168**, 027505 (2021).
201. G. Li and D. Wen, *Chin. Chem. Lett.*, **32**, 221 (2021).
202. C. Moonla, S. Jankhunthod, and K. Ngamchuea, *J. Electrochem. Soc.*, **168**, 116507 (2021).
203. C. Dagdeviren et al., *Proc. Natl Acad. Sci.*, **111**, 1927 (2014).
204. I. Jeerapan and N. Ma, *C*, **5**, 62 (2019).
205. R. D. I. G. Dharmasena and S. R. P. Silva, *Nano Energy*, **62**, 530 (2019).
206. I. Jeerapan, J. R. Sempionatto, and J. Wang, *Adv. Funct. Mater.*, **30**, 1906243 (2020).
207. I. Hochmair, P. Nopp, C. Jolly, M. Schmidt, H. Schöber, C. Garnham, and I. Anderson, *Trends in Amplification*, **10**, 201 (2006).
208. T. Saidi, O. Zaim, M. Moufid, N. El Bari, R. Ionescu, and B. Bouchikhi, *Sensors Actuators B*, **257**, 178 (2018).
209. D. Elleri, D. B. Dunger, and R. Hovorka, *BMC Medicine*, **9**, 120 (2011).
210. N. Ha, K. Xu, G. Ren, A. Mitchell, and J. Z. Ou, *Advanced Intelligent Systems*, **2**, 2000063 (2020).
211. Y. Xu, C. Li, Y. Jiang, M. Guo, Y. Yang, Y. Yang, and H. Yu, *J. Electrochem. Soc.*, **167**, 047508 (2020).
212. R. Fan, Y. Li, K.-W. Park, J. Du, L. H. Chang, E. R. Strieter, and T. L. Andrew, *ECS Sensors Plus*, **1**, 010601 (2022).